PROJECT REPORT

ON

DIELECTRIC RESONATOR ANTENNA

Submitted in partial fulfillment of the Degree of

Bachelor of Technology

May-2014

Submitted by

Dhruv Batra (101002)

Amit kumar ojha (101007)

Aman kumar (101027)

Under the guidance of

Prof. Dr. Ghanshyam singh

DEPARTMENT OF ELECTRONICS AND COMMUNICATION ENGINEERING
JAYPEE UNIVERSITY OF INFORMATION TECHNOLOGY, WAKNAGHAT-173234

Certificate

This is to certify that project report entitled "**DIELECTRIC RESONATOR ANTENNA**", submitted by Dhruv Batra(101002),Amit Kumar Ojha(101007) and Aman Kumar(101027) in partial fulfillment for the award of degree of Bachelor of Technology in Electronics and Communication Engineering to Jaypee University of Information Technology, Waknaghat, Solan has been carried out under my supervision.

This work has not been submitted partially or fully to any other University or Institute for the award of this or any other degree or diploma.

Date:

Supervisor's Name:

Prof. Dr. Ghanshyam Singh

Dept. of ECE, JUIT

ACKNOWLEDGEMENT

We owe a great many thanks to a great many people who have helped and supported us during this project. Our deepest thanks to **Dr. Ghanshyam Singh**, our project guide for his exemplary guidance, monitoring and constant encouragement throughout the course of this project work. He has taken great pains to go through the project and make necessary corrections as and whenever needed. We are also grateful to **Mr. Mohan Sharma (ECE Project lab**) for his practical help and guidance. We would also like to thank all the faculty members of ECE department without whom the progress of this project would have been a distant reality. We also extend our heartfelt thanks to our family and well-wishers.

Date:

Name of the students:

Dhruv Batra (101002)

Amit Kumar Ojha (101007)

Aman Kumar (101027)

SUMMARY

The DRA is an open resonating structure, fabricated from a low loss microwave dielectric material. Dielectric resonators (DR's) have proved themselves to be ideal candidates for antenna applications by virtue of their high radiation efficiency, flexible feed arrangement, simple geometry, small size and the ability to produce different radiation pattern using different modes. Feeding techniques like probe feed, aperture slot, microstrip line and coplanar line can be used with the DRAs, which enables them for integration with microwave printed technology.

The Aim of my project is developing a Dielectric Resonator Antenna (DRA) antenna which transmits 'radio waves' through a transmitter which are received by the FM radio and produce the output.

TABLE OF CONTENTS

LIST OF FIGURES

CHAPTER 1:INTRODUCTION TO ANTENNAS

Our project focuses on the hardware fabrication and software simulation of several antennas. In order to completely understand the above it is necessary to start off by understanding various terms associated with antennas and the various types of antennas. This is what is covered in this introductory chapter.

1.1 ANTENNA PARAMETERS

An antenna is an electrical conductor or system of conductors .

Transmitter - Radiates electromagnetic energy into space .

Receiver - Collects electromagnetic energy from space .

The IEEE definition of an antenna as given by Stutzman and Thiele is, “That part of a transmitting or receiving system that is designed to radiate or receive electromagnetic waves”. The major parameters associated with an antenna are defined in the following sections.

1.1.1 Antenna Gain

Gain is a measure of the ability of the antenna to direct the input power into radiation in a particular direction and is measured at the peak radiation intensity. Consider the power density radiated by an isotropic antenna with input power P_0 at a distance R which is given by $S = P_0/4\pi R^2$. An isotropic antenna radiates equally in all directions, and its radiated power density S is found by dividing the radiated power by the area of the sphere $4\pi R^2$. An isotropic radiator is considered to be 100% efficient. The gain of an actual antenna increases the power density in the direction of the peak radiation:

$$S = \frac{P_0 G}{4\pi R^2} = \frac{|\mathbf{E}|^2}{\eta} \quad \text{or} \quad |\mathbf{E}| = \frac{1}{R}\sqrt{\frac{P_0 G \eta}{4\pi}} = \sqrt{S\eta}$$

Gain is achieved by directing the radiation away from other parts of the radiation sphere. In general, gain is defined as the gain-biased pattern of the antenna.

$$S(\theta, \phi) = \frac{P_0 G(\theta, \phi)}{4\pi R^2} \qquad \text{power density}$$

$$U(\theta, \phi) = \frac{P_0 G(\theta, \phi)}{4\pi} \qquad \text{radiation intensity}$$

1.1.2 Antenna Efficiency

The surface integral of the radiation intensity over the radiation sphere divided by the input power P_0 is a measure of the relative power radiated by the antenna, or the antenna efficiency.

$$\frac{P_r}{P_0} = \int_0^{2\pi} \int_0^{\pi} \frac{G(\theta, \phi)}{4\pi} \sin\theta \, d\theta \, d\phi = \eta_e \qquad \text{efficiency}$$

where *Pr* is the radiated power. Material losses in the antenna or reflected power due to poor impedance match reduce the radiated power.

1.1.3 Effective Area

Antennas capture power from passing waves and deliver some of it to the terminals. Given the power density of the incident wave and the effective area of the antenna, the power delivered to the terminals is the product

$$P_d = SA_{\text{eff}}$$

For an aperture antenna such as a horn, parabolic reflector, or flat-plate array, effective area is physical area multiplied by aperture efficiency. In general, losses due to material, distribution, and mismatch reduce the ratio of the effective area to the physical area. Typical estimated aperture efficiency for a parabolic reflector is 55%. Even antennas with infinitesimal physical areas, such as dipoles, have effective areas because they remove power from passing waves.

1.1.4 Directivity

Directivity is a measure of the concentration of radiation in the direction of the maximum.

$$\text{directivity} = \frac{\text{maximum radiation intensity}}{\text{average radiation intensity}} = \frac{U_{\max}}{U_0}$$

Directivity and gain differ only by the efficiency, but directivity is easily estimated from patterns. Gain—directivity times efficiency—must be measured.

The average radiation intensity can be found from a surface integral over the 2 radiation sphere of the radiation intensity divided by 4π, the area of the sphere in steradians:

$$\text{average radiation intensity} = \frac{1}{4\pi}\int_0^{2\pi}\int_0^{\pi} U(\theta, \phi)\sin\theta\, d\theta\, d\phi = U_0$$

This is the radiated power divided by the area of a unit sphere. The radiation intensity $U(\theta,\varphi)$ separates into a sum of co- and cross-polarization components:
Both co- and cross-polarization directivities can be defined:

$$\text{directivity}_{\text{C}} = \frac{U_{\text{C,max}}}{U_0} \qquad \text{directivity}_{\times} = \frac{U_{\times,\text{max}}}{U_0}$$

Directivity can also be defined for an arbitrary direction $D(\theta,\varphi)$ as radiation intensity divided by the average radiation intensity, but when the coordinate angles are not specified, we calculate directivity at $U_{\max}$.

1.1.5 Path Loss

We combine the gain of the transmitting antenna with the effective area of the receiving antenna to determine delivered power and path loss. The power density at the receiving antenna is given by equation 1.2 and the received power is given by equation 1.4. By combining the two, we obtain the path loss as given below.

$$\frac{P_d}{P_t} = \frac{A_2 G_1(\theta, \phi)}{4\pi R^2}$$

Antenna 1 transmits, and antenna 2 receives. If the materials in the antennas are linear and isotropic, the transmitting and receiving patterns are identical . When we consider antenna 2 as the transmitting antenna and antenna 1 as the receiving antenna, the path loss is

$$\frac{P_d}{P_t} = \frac{A_1 G_2(\theta, \phi)}{4\pi R^2}$$

We make quick evaluations of path loss for various units of distance *R* and for frequency

1.1.6 Input Impedance

The input impedance of an antenna is defined as "the impedance presented by an antenna at its terminals or the ratio of the voltage to the current at the pair of terminals or the ratio of the appropriate components of the electric to magnetic fields at a point". Hence the impedance of the antenna can be written as given below.

$$Z_{in} = R_{in} + jX_{in}$$

where ;

Z_{in} is the antenna impedance at the terminals

R_{in} is the antenna resistance at the terminals

X_{in} is the antenna reactance at the terminals

The imaginary part, X_{in} of the input impedance represents the power stored in the near field of the antenna. The resistive part, R_{in} of the input impedance consists of two components, the radiation resistance R_r and the loss resistance R_L. The power associated with the radiation resistance is the power actually radiated by the antenna, while the power dissipated in the loss resistance is lost as heat in the antenna itself due to dielectric or conducting losses.

1.1.7 Antenna Factor

The engineering community uses an antenna connected to a receiver such as a spectrum analyzer, a network analyzer, or an RF voltmeter to measure field strength E. Most of the time these devices have a load resistor ZL that matches the antenna impedance.
The incident field strength E_i equals antenna factor AF times the received voltage V_{rec}.
We relate this to the antenna effective height:

$$\mathrm{AF} = \frac{E_i}{V_{\mathrm{rec}}} = \frac{2}{h}$$

AF has units meter^{-1} but is often given as dB(m^{-1}). Sometimes, antenna factor is referred to the open-circuit voltage and it would be one-half the value given by equation 1.11. We assume that the antenna is aligned with the electric field; in other words, the antenna polarization is the electric field component measured:

$$\mathrm{AF} = \sqrt{\frac{\eta}{Z_L A_{\mathrm{eff}}}} = \frac{1}{\lambda}\sqrt{\frac{4\pi}{Z_L G}}$$

This measurement may be corrupted by a poor impedance match to the receiver and any cable loss between the antenna and receiver that reduces the voltage and reduces the calculated field strength.

1.1.8 Return Loss

It is a parameter which indicates the amount of power that is "lost" to the load and does not return as a reflection. Hence the RL is a parameter to indicate how well the matching between the transmitter and antenna has taken place. Simply put it is the S11 of an antenna. A graph of s11 of an antenna vs frequency is called its return loss curve. For optimum working such a graph must show a dip at the operating frequency and have a minimum dB value at this frequency. This parameter was found to be of crucial importance to our project as we sought to adjust the antenna dimensions for a fixed operating frequency (say 1.9 GHz). A simple RL curve is shown in figure

1.1.9 Radiation Pattern

The radiation pattern of an antenna is a plot of the far-field radiation properties of an antenna as a function of the spatial co-ordinates which are specified by the elevation angle (θ) and the azimuth angle (φ). More specifically it is a plot of the power radiated from an antenna per unit solid angle which is nothing but the radiation intensity. It can be plotted as a 3D graph or as a 2D polar or Cartesian slice of this 3D graph. It is an extremely parameter as it shows the antenna's directivity as well as gain at various points in space. It serves as the signature of an antenna and one look at it is often enough to realize the antenna that produced it.

Because this parameter was so important to our software simulations we needed to understand it completely. For this purpose we obtained the 2D polar plots of radiation patterns for a few antennas in our lab using a ScienTech antenna trainer kit

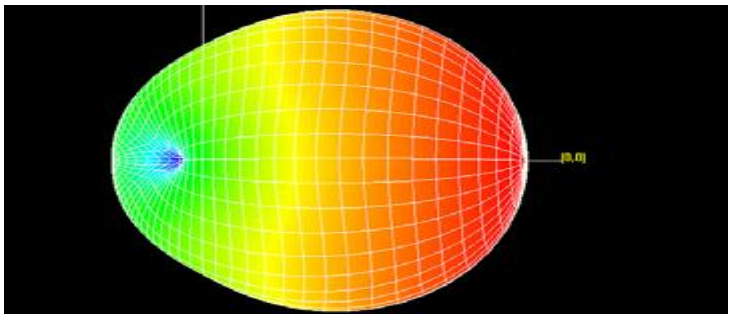

Figure 1.1:- 3D Radiation Pattern

1.1.10 Beamwidth

Beamwidth of an antenna is easily determined from its 2D radiation pattern and is also a very important parameter. Beamwidth is the angular separation of the half-power points of the radiated pattern. The way in which beamwidth is determined is shown in figure 1.2.

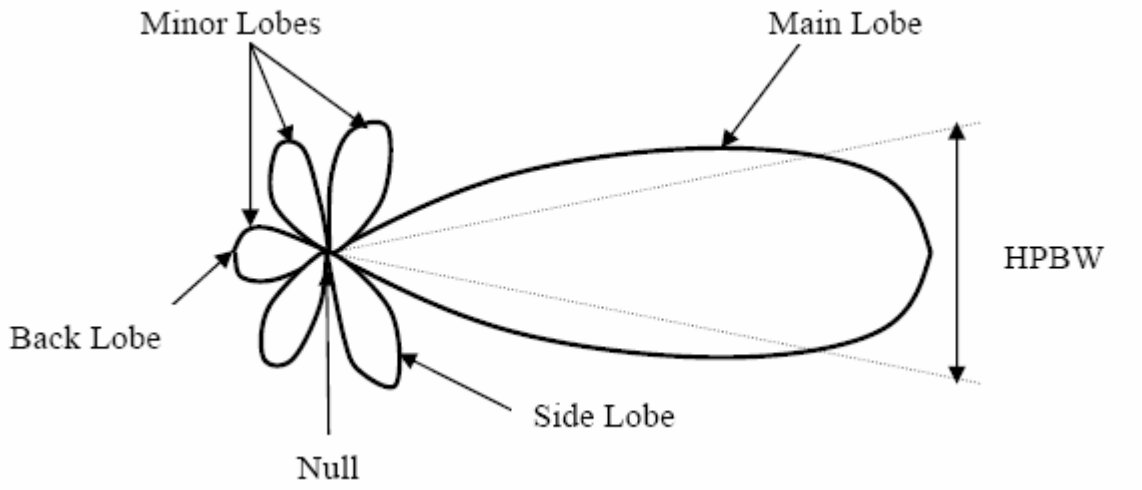

Figure 1.2

1.2 TYPES OF ANTENNAS

Antennas can be classified in several ways. One way is the frequency band of operation. Others include physical structure and electrical/electromagnetic design. Most simple, non-directional antennas are basic dipoles or monopoles. More complex, directional antennas consist of arrays of elements, such as dipoles, or use one active and several passive elements, as in the Yagi antenna. New antenna technologies are being developed that allow an antenna to rapidly change its pattern in response to changes in direction of arrival of the received signal. These antennas and the supporting technology are called adaptive or "smart" antennas and may be used for the higher frequency bands in the future. A few commonly used antennas are described in the following sections.

1.2.1 Dipoles and Monopoles

The vertical dipole—or its electromagnetic equivalent, the monopole—could be considered one of the best antennas for LMR applications. It is omni directional (in azimuth) and, if it is a half-wavelength long, has a gain of 1.64 (or G = 2.15 dBi) in the

horizontal plane. Although this is a simple antenna, it can be difficult to mount on a mast or vehicle. It is half a dipole placed in half space, with a perfectly conducting, infinite surface at the boundary.

1.2.2 Corner Reflector

An antenna comprised of one or more dipole elements in front of a corner reflector, called the corner-reflector antenna.

1.2.3 Yagi Antenna

Another antenna design that uses passive elements is the Yagi antenna. This antenna, is inexpensive and effective. It can be constructed with one or more (usually one or two) reflector elements and one or more (usually two or more) director elements.

CHAPTER 2:LENS ANTENNAS

Lens antennas are, not surprisingly, antenna systems where the radiation characteristics of a feed are modified by the use of a lens. For microwave engineers, the term ‘lens’ is more encompassing than in common usage. As well as traditional dielectric lenses, any structure that converges or diverges a wave is considered a lens. This includes arrays of antenna elements, which selectively advance or delay portions of the wave’s phase front. The simplest design of any focusing lens can be performed using ray tracing and metric optics. The lens is designed to create equal electrical path lengths between a focal point and a planar wavefront. Since an array lens is discretized into elements, the electrical path length is designed to be equal for each element.

2.1 DIELECTRIC LENSES

At microwave frequencies, dielectric lenses can be created from traditional bulk materials or artificial materials. Traditional artificial dielectrics consist of a lattice of discrete metal particles, e.g., metal strips, rods, or spheres More recent artificial materials, known as meta-materials, also consist of a metallic lattice; however, they can synthesize properties that are not commonly found in nature. The lattice spacing is much larger than the atomic structure of a bulk material dielectric, but smaller than a wavelength.

2.2 APPLICATIONS OF DIELECTRIC ANTENNAS

Many contemporary technical applications
crash avoidance systems,
imaging systems,
base stations for wireless communication systems
require antennas capable of supporting several radio links at the same time.
Favourable solutions for such scenarios are dielectric lens antennas

2.3 ADVANTAGES AND DISADVANTAGES OF DIELECTRIC ANTENNAS

They offer a high degree of flexibility and versatility over a wide frequency range,

allowing for designers to suit many requirements.

DRAs offer the following advantages:

¾ DRAs come in simple geometries like circular cylinder, hemisphere, rectangular etc. are readily available and can be easily fabricated.

¾ The DRA size is proportional to 0

Thus for a particular same frequency there is a natural reduction in size, compared with their conventional counterparts like microstrip antennas. Also, different values of εr (ranging from 4 to 100) can be used, thus allowing the designer the flexibility in controlling the size and bandwidth.

2.4 SIMULATION SOFTWARE – HFSS

HFSS is a commercial finite element method solver for electromagnetic structures from Ansys. The acronym originally stood for **high frequency structural simulator**. It is one of several commercial tools used for antenna design, and the design of complex RF electronic circuit elements including filters, transmission lines, and packaging. It was originally developed by Professor Zoltan Cendes and his students at Carnegie Mellon University

2.4.1 DESIGN OF A SIMPLE RECTANGULAR WAVEGUIDE

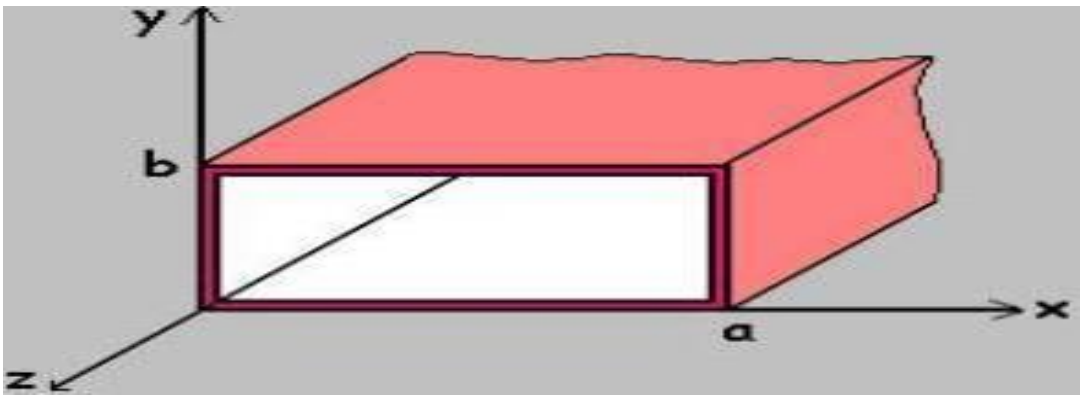

Figure 2.1

OBJECTIVE.

Using HFSS, to simulate a rectangular waveguide.

To obtain the Field patterns, for the first four modes.

Sweep frequency from 1 – 21 GHz.

To generate wavelength v/s frequency graphs.

Material Selection.

electing the medium to be a Vacuum

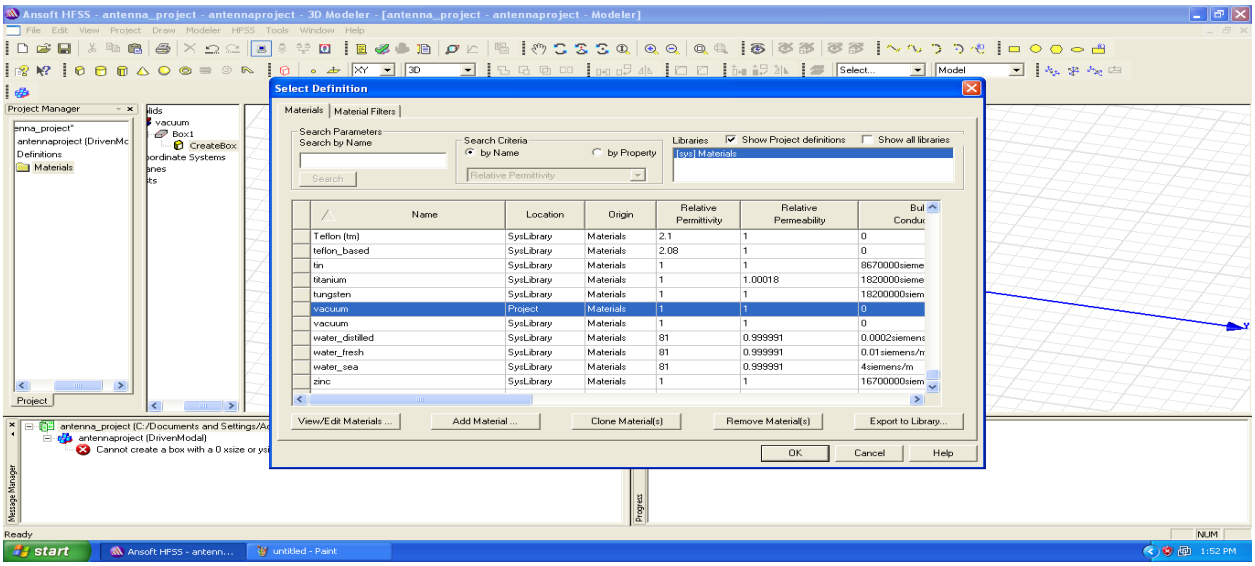

Figure 2.2

Assigning the Faces, which are to be processed

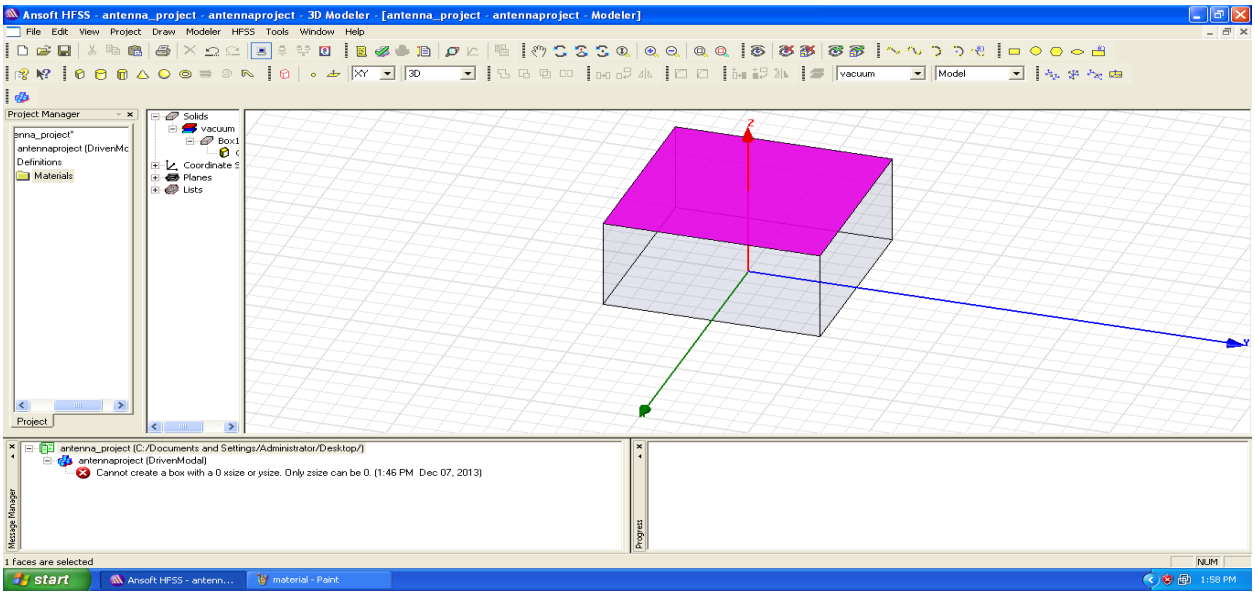

Figure 2.3

Setting the Boundary Conditions

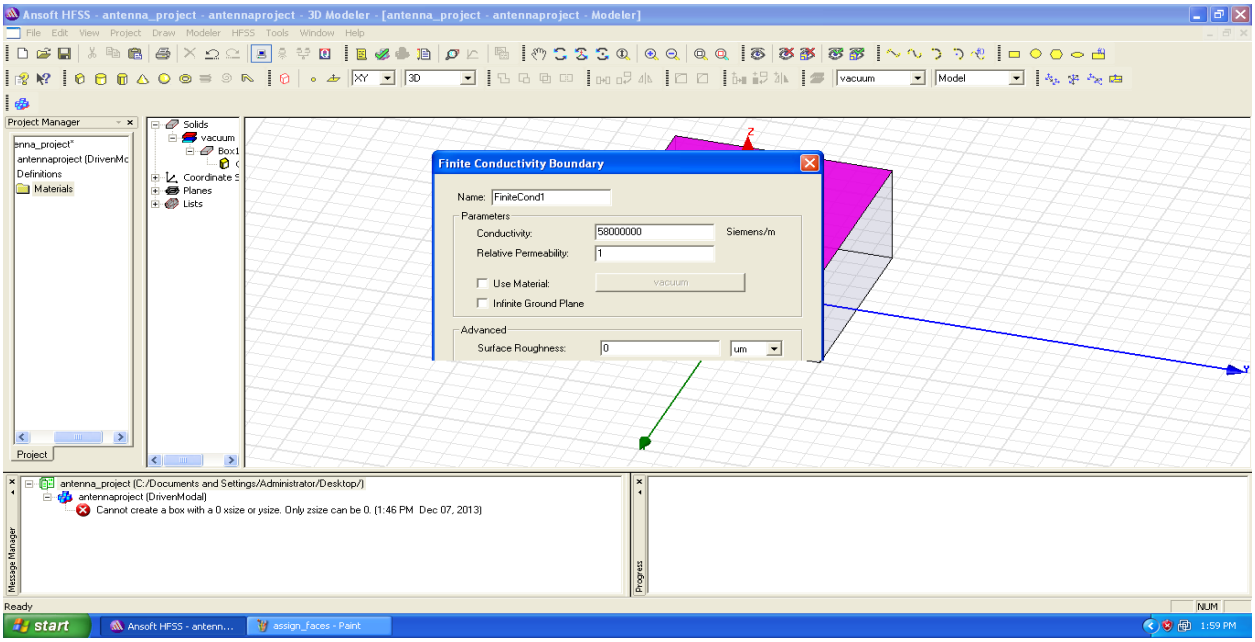

Figure 2.4

Selecting the Integration Line

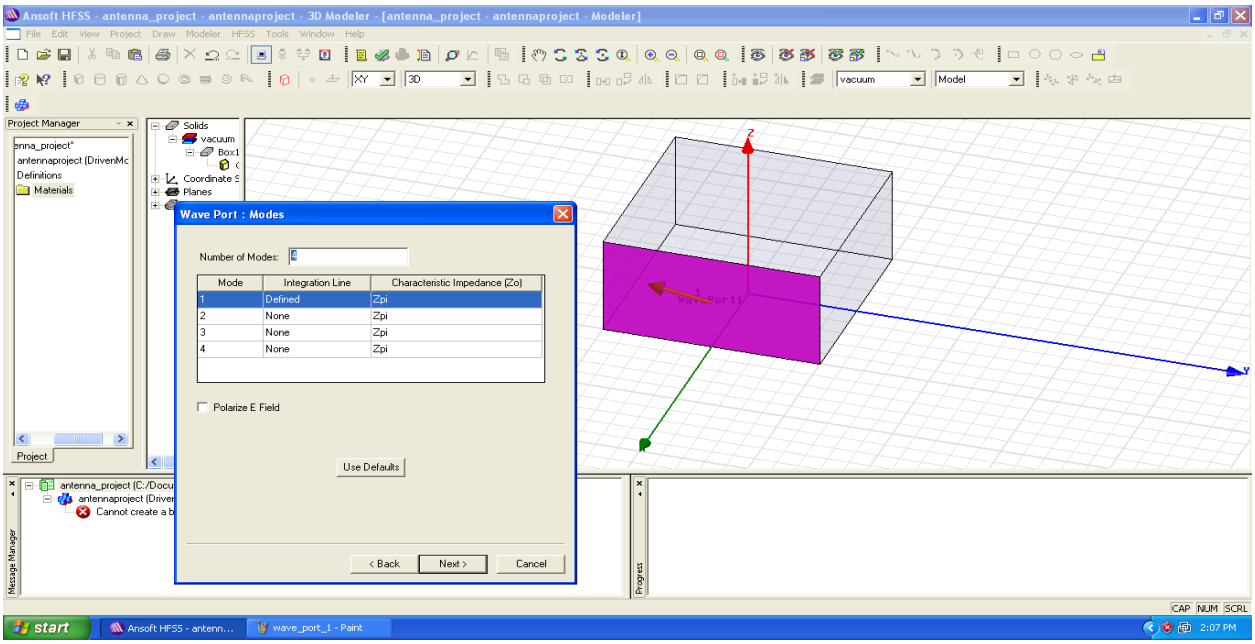

Figure 2.5

The Solution Setup

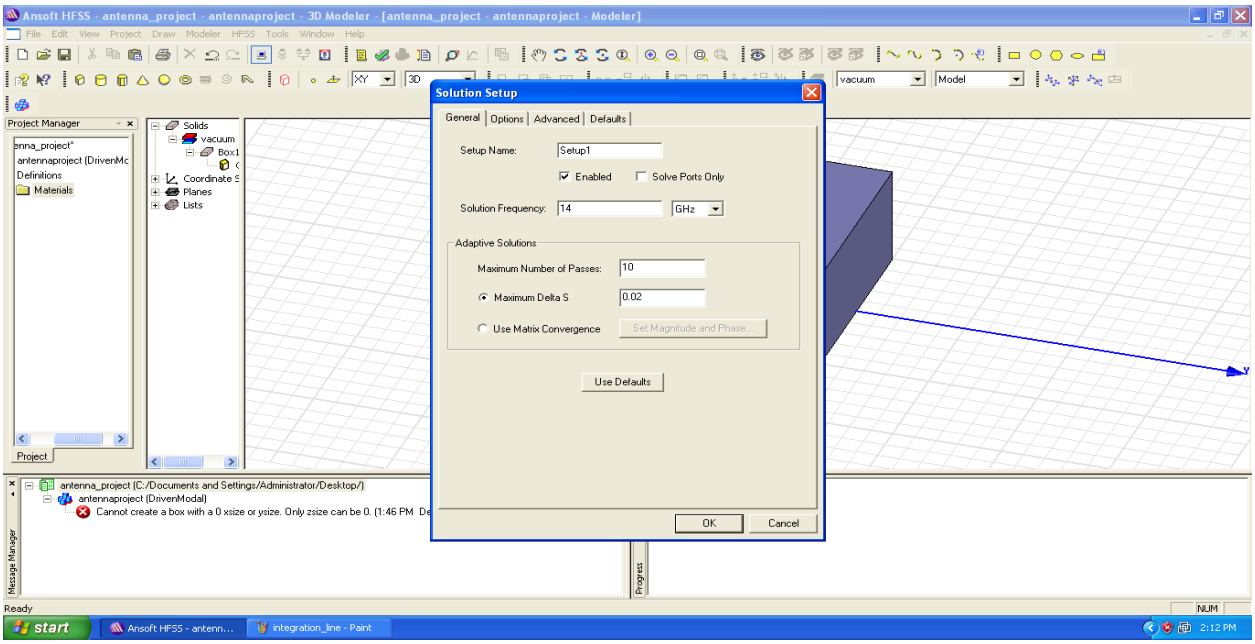

Figure 2.6

Setting the Frequency Sweep.

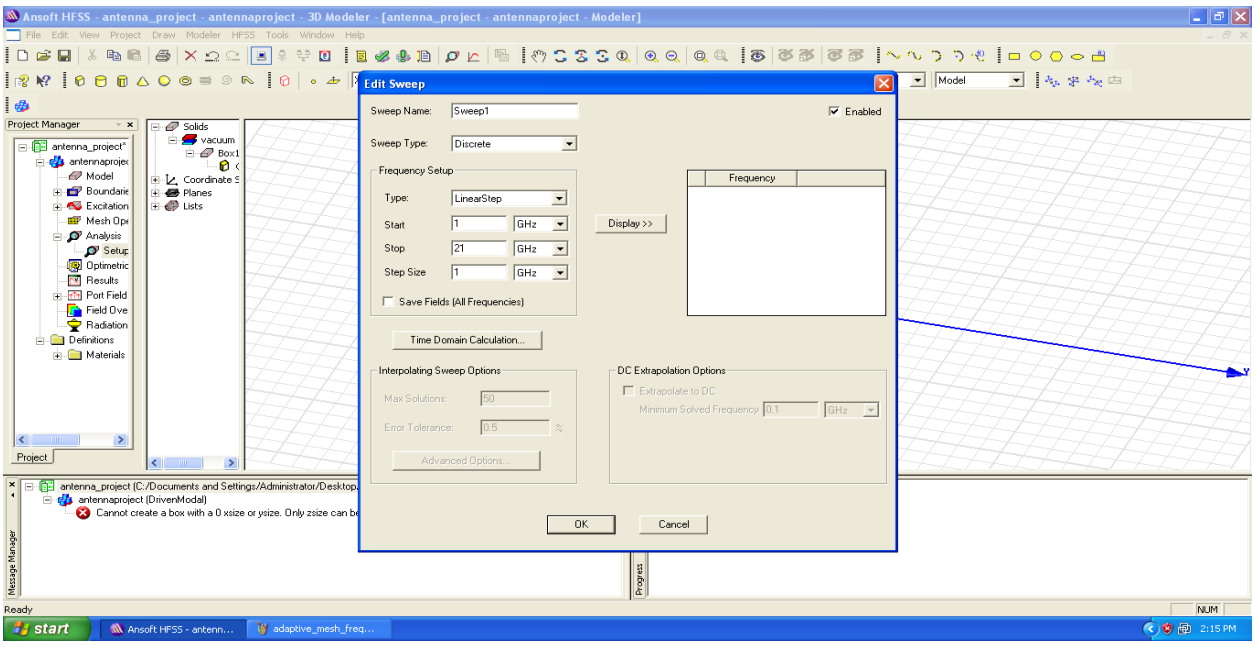

Figure 2.7

Analysis

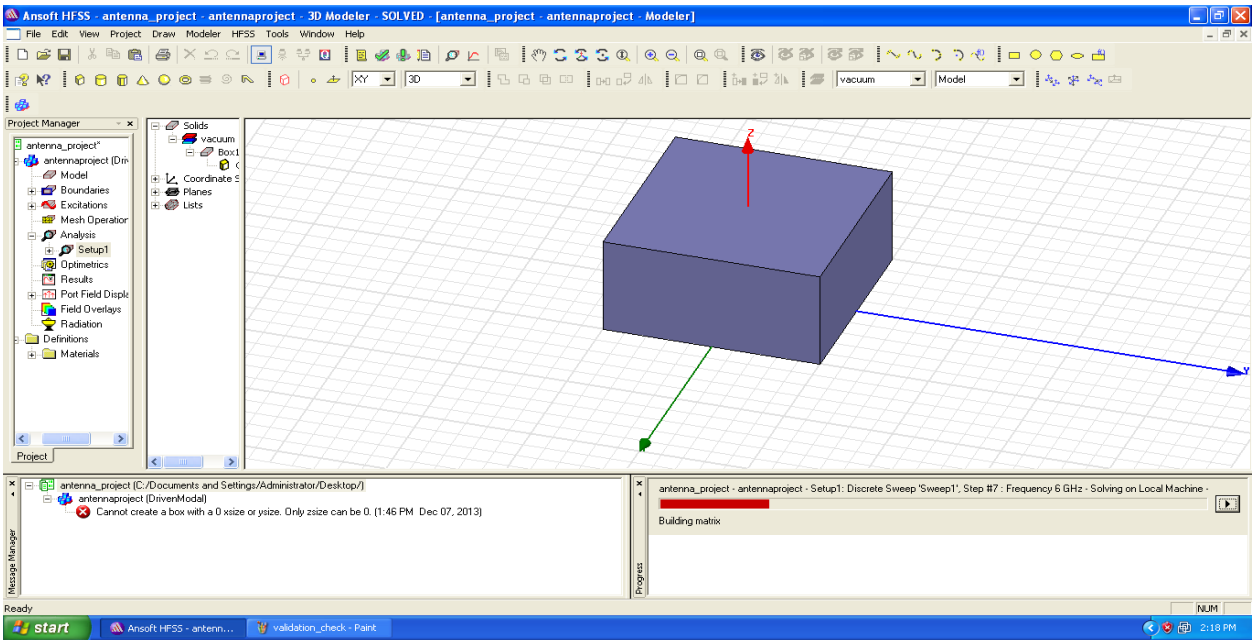

Figure 2.8

Validation Check.

Result – Successful.

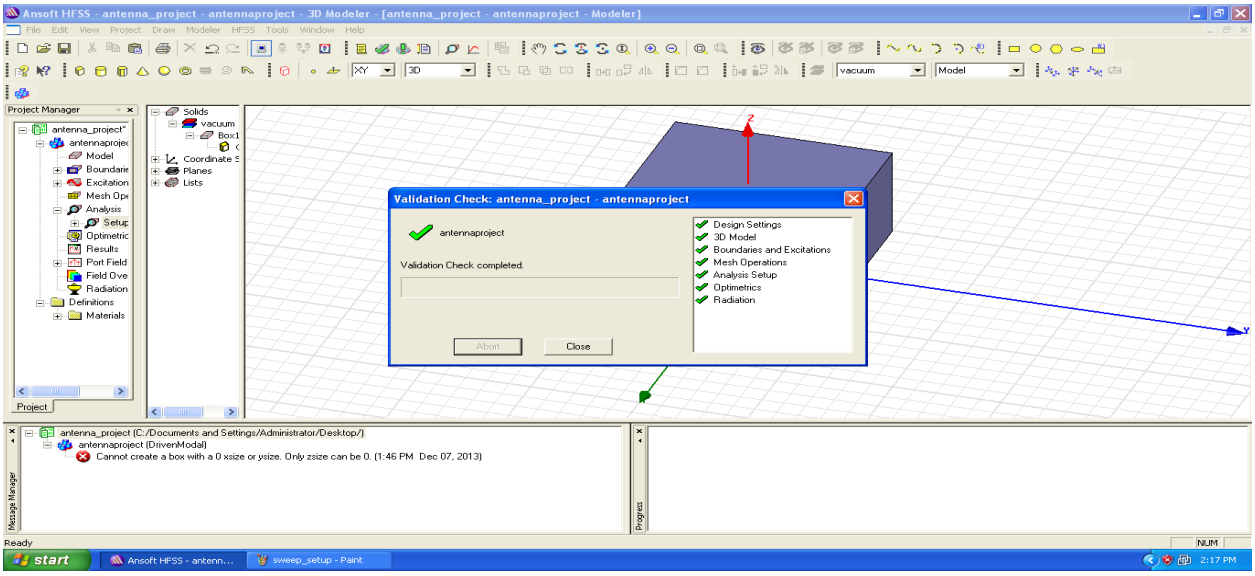

Figure 2.9

Solution Data.

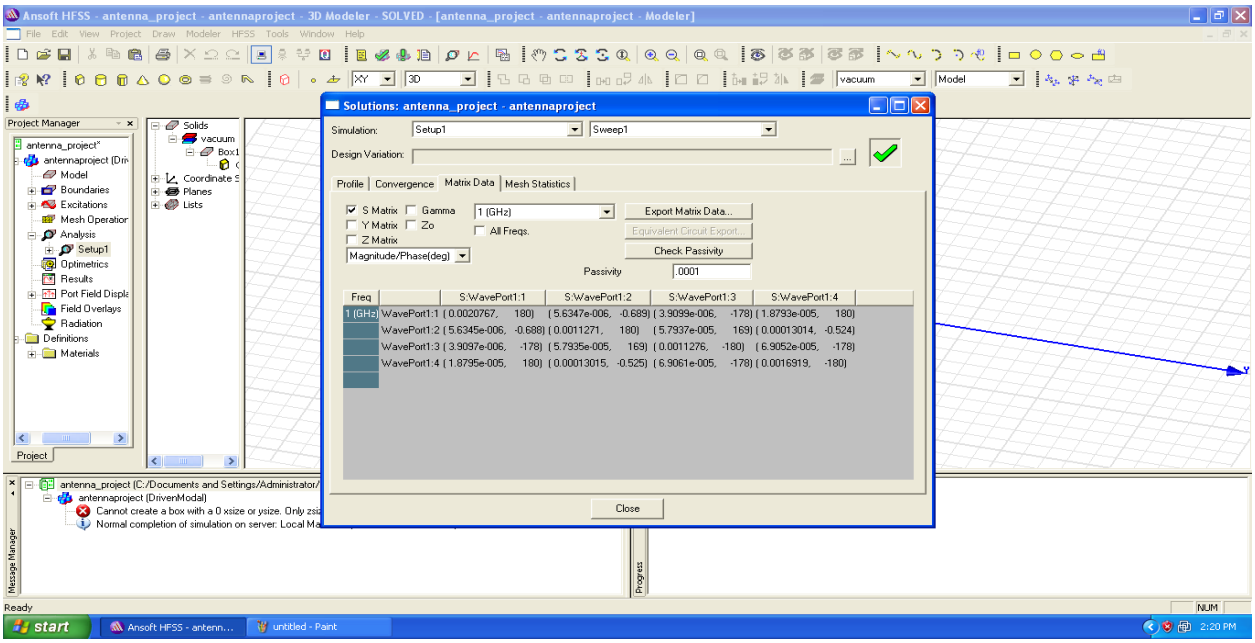

Figure 2.10

Electric Field Display.

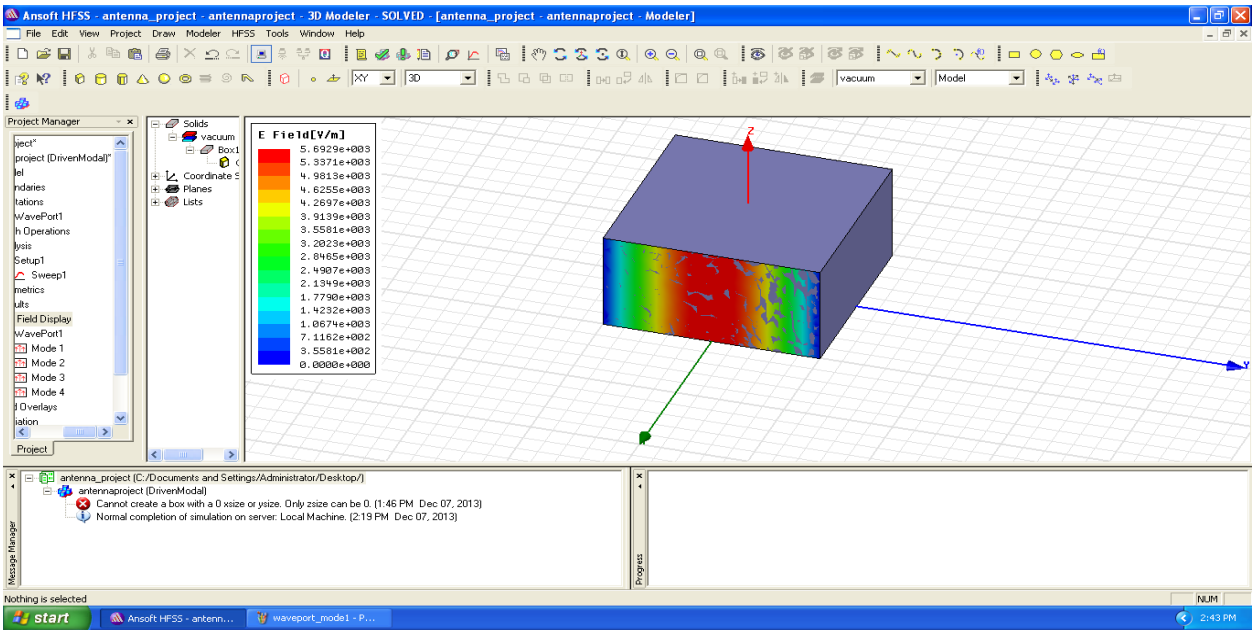

Figure 2.11

Electric and Magnetic Fields Display

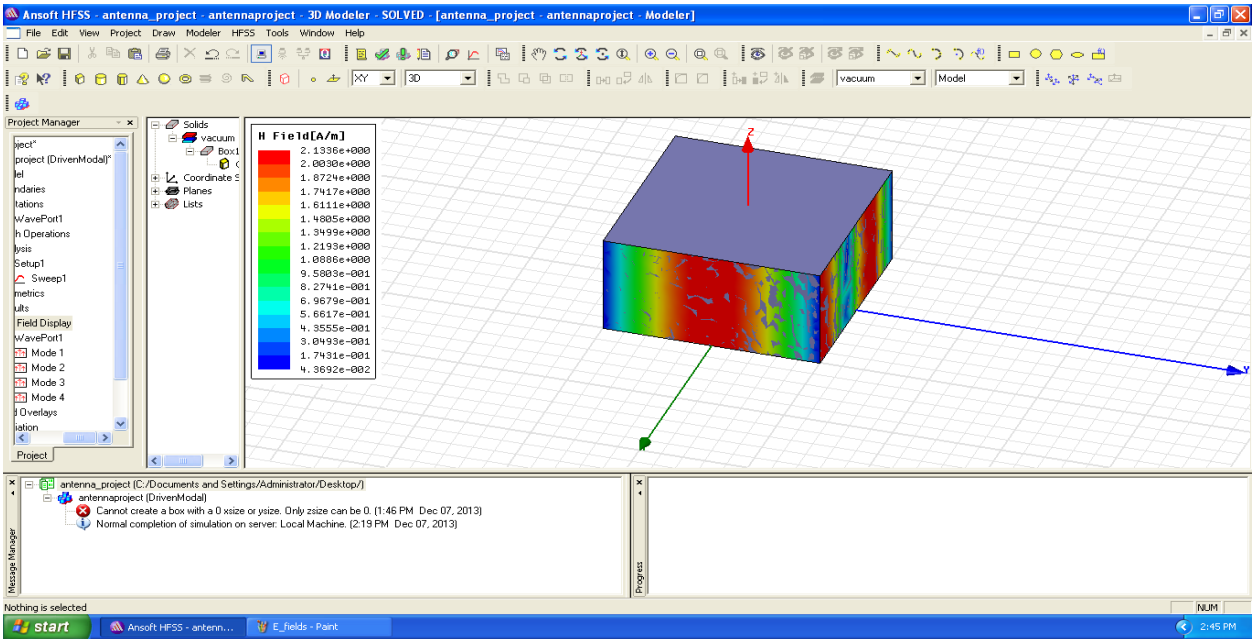

Figure 2.12

CHAPTER 3: DIELECTRIC RESONATOR ANTENNA

The DRA is an open resonating structure, fabricated from a low loss microwave dielectric material. Dielectric resonators (DR's) have proved themselves to be ideal candidates for antenna applications by virtue of their high radiation efficiency, flexible feed arrangement, simple geometry, small size and the ability to produce different radiation pattern using different modes. Feeding techniques like probe feed, aperture slot, microstrip line and coplanar line can be used with the DRAs, which enables them for integration with microwave printed technology.

Additionally, DRA's avoid some limitations of the patch antenna including the high conductor losses at millimeter-wave frequencies, sensitivity to tolerances, and narrow bandwidth. DRA's of cylindrical, hemispherical and rectangular shapes are mostwidely used and investigated. The rectangular shape is much easier to fabricate and oneor more dimensional parameters are available as additional degrees of freedom for thedesign . Impedance bandwidth varies over a wide range with resonator parameters. Itcan be as small as a few percent with high 8_r material or over 20 % with small 8_r in conjunction with certain geometries and resonant modes. Different far field radiation patterns are supported. For a given DRA geometry, the radiation pattern can be made to change by exciting different modes.

Systematic experimental investigations on dielectric resonator antennas (DRA's) were first carried out by Long *et al.*. Since then, theoretical and experimental investigations have been reported by many investigators on DRA's of various shapes such as spherical, cylindrical (or cylindrical ring), rectangular, etc. DRAs with various other shapes are also reported in different literature.

3.1 ADVANTAGES OF DRA

DRAs offer a high degree of flexibility and versatility over a wide frequency range, allowing for designers to suit many requirements. DRAs offer the following advantages:

> DRAs come in simple geometries like circular cylinder, hemisphere, rectangular etc. are readily available and can be easily fabricated.

> The DRA size is proportional to ~*j*=, where A_0 is the wavelength at resonant

frequency and 8_r is the dielectric constant of the DR. Thus for the same frequency there is a natural reduction in size, compared with their conventional counterparts like microstrip antennas. Also, different values of 8r (ranging from 4 to 100) can be used, thus allowing the designer the flexibility in controlling the size and bandwidth.

> Depending on the resonator shape, various modes can be excited within the DRA element. These modes can produce different radiation patterns for various coverage requirements. Also, the Q-factor of some of these modes will depend on the aspect ratio of the DRA, thus allowing one more degree of flexibility in the design.
> Many of the existing feeding schemes can be used (slots, probes, microstrip, coplanar waveguides, dielectric image guide, etc.). This makes them easy to integrate with existing technologies.
> Compared with the microstrip antenna, DRA has a much wider impedance bandwidth. This is because the microstrip antenna radiates only through two narrow radiation slots, whereas the DRA radiates through the whole antenna surface except the grounded part. Moreover the operating bandwidth of a DRA can be varied by suitably choosing the dielectric constant of the resonator material and its dimensions.
> DRAs have been designed to operate over a wide frequency range (1 GHz to 44 GHz) compared with other antennas existing in the literature.
> DRAs have a high dielectric strength and hence higher power handling capacity. Moreover the temperature-stable ceramics enable the antenna to operate in a wide temperature range.
> There is no inherent conductor loss for a DRA. High radiation efficiency is thus possible in case of DR antennas. It is especially attractive for high frequency millimeter wave applications, where the loss from metallic antennas can be high.

3.2 RECTANGULAR DRA

Rectangular DRAs offer practical advantages over cylindrical and spherical shape. For example, the mode degeneracy can be avoided in the case of rectangular DRA's by properly choosing the three dimensions of the resonator. It may be noted that mode degeneracy always exists in the case of a spherical DRA and in the case of hybrid modes of a cylindrical DRA. The mode degeneracy can enhance the cross-polar levels of an antenna, thus limiting its performance. Further, for a given resonant frequency, two aspect ratios of a rectangular DRA (height/length and width/length) can be chosen

independently. Since the bandwidth of a DRA also depends on its aspect ratio(s), a rectangular-shaped DRA provides more flexibility in terms of bandwidth control .

A rectangular DRA support two type modes, TM and TE, but TM modes have never been observed experimentally. Therefore the existence of TM modes appears to be doubtful. Figure 1.1 shows a rectangular DRA with the corresponding coordinate system. The resonant modes can be TE to either dimension, denoted as TE^x, TE^y, or TE^z. A rectangular DR has three independent dimensions. The modes of a DR can therefore, be TE to any of three dimensions.

Referring to the DR and co-ordinates system shown in figure 1.1, the modes with lowest order indexes are TE^z_{111}, TE^y_{111} and TE^x_{111}. If the dimensions of the DR are such that a > b > d, the modes in the order of increasing resonant frequency are TE_{111}, TE^y_{101} and TE^x_{011}. The analysis of all the modes is similar. For example, for TE mode, the analysis for the field components inside the resonator can be done from the directed magnetic potential <*P*

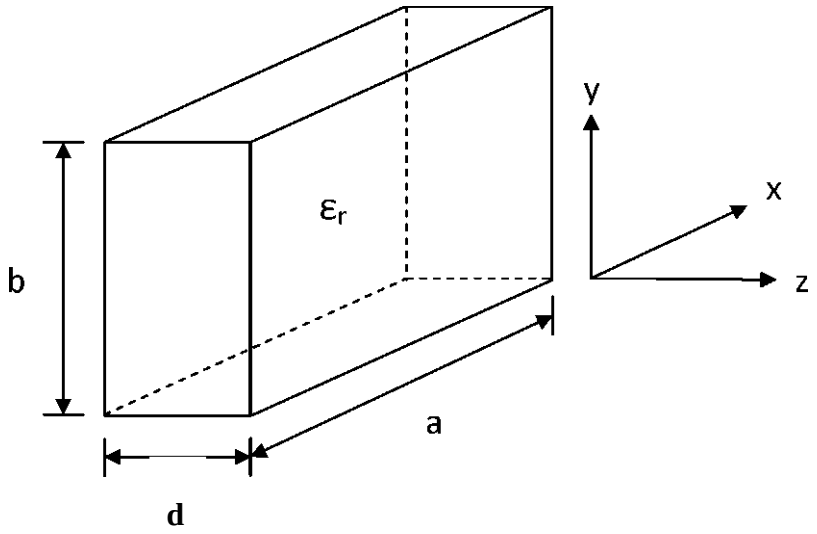

Figure 3.1: Isolated rectangular DRA.

$$H_z = -A\cos(k_x x)\cos(k_y y)\cos(k_z z) \quad (1)$$

$$H_x = -A\sin(k_x x)\cos(k_y y)\sin(k_z z) \quad (2)$$

$$H_Y = A\cos(k_x x)\sin(k_y y)\,\mathrm{sm}(k_z z) \quad (3)$$

where*A* is an arbitrary constant and k_x, k_y, and k_z denote the wavenumbers along

the x, y, and z directions, respectively, inside the DR.

$$K\tan[^{kd}] = (r-1)k\,(0^2-k^2) \qquad (4)$$

The dimensions of the radiating portion of the DR were determined using the equation (4) developed for the dielectric waveguide model (DWM) for a rectangular resonator in free-space where

$$Q = \wedge_{rad} \qquad (5)$$

$$K = {}^{n};\ k_y = {}^{n};\ K = \ \wedge;\ C = \ 3\ \mathbf{x}10^8 m / S \qquad (6)$$

Figure shows the rectangular resonator with length a, breadth b and height d. Resonances can occur at the following frequencies

Where e is the permittivity, (i is the material permeability, and m, n and p are integers. In this configuration, TEx011 mode is the dominant mode, because it occurs at the lowest frequency at which a cavity resonance can exist. From equation (10) it can be seen that the frequency at which this dominant resonant mode can exists (the cutoff frequency) is inversely proportional to the square root of the product of material parameters, e.

3.3.DIFFERENT FEED TECHNIQUES FOR DR

Electromagnetic power can be coupled to the DR in several ways. These coupling mechanisms can have a significant impact on the resonant frequency and Q-factor. Numerous feeding techniques are available in the literature. Some of the commonly used techniques are,

3.4 SLOT/APERTURE COUPLING

Figure below depicts a DRA fed by an aperture. The aperture behaves like a magnetic current running parallel to the length of the slot, which excites the magnetic fields in the DRA. The aperture consists of a slot cut in a ground plane and fed by a microstrip line beneath the ground plane. This coupling mechanism has the advantage of having the feed network located below the ground plane, thus avoiding spurious radiation. The microstrip stub can be designed to cancel out the reactive component of the slot, thus allowing for an impedance match to the DRA. Moreover, slot coupling is an attractive method for integrating DRAs with printed feed structures .The coupling level can be adjusted by moving the DRA with respect to the slot.

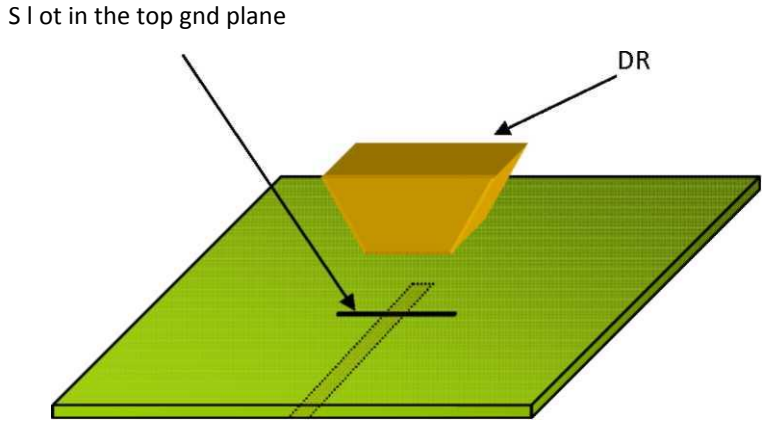

Figure 3.2: Slot fed DRA

3.5 COAXIAL PROBE COUPLING

The coaxial probe can either be located adjacent to the DRA or can be embedded within it. The amount of coupling can be optimized by adjusting the probe height and the DRA location. Also, depending on the location of the probe, various modes can be excited. For the probe located adjacent to the DRA, the magnetic fields of the $TE_{11}5$ mode of the rectangular DRA are excited (which radiate like a horizontal magnetic dipole). For a probe located in the centre of a cylindrical DRA, the TE_{011}mode is excited (radiating like a vertical dipole). Another advantage of using probe coupling is that one can couple directly into a 50Q system, without the need for a matching

network. Probes are useful at lower frequencies where aperture coupling may not be practical due to the large size of the slot requited.

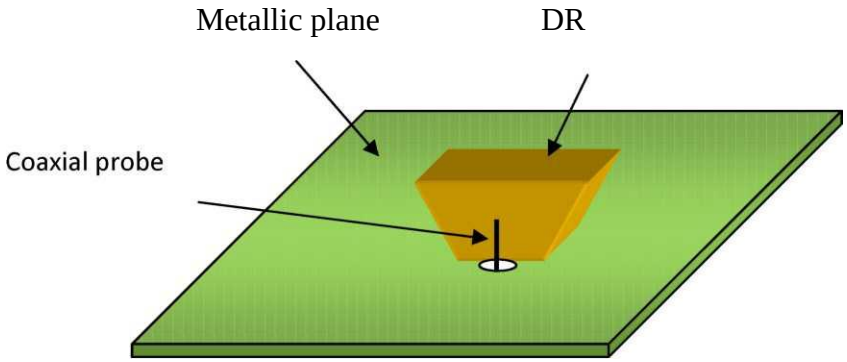

Figure 3.3: Coaxial probe fed DRA

3.6 MICROSTRIP TRANSMISSION LINE / PROXIMITY COUPLING

Another common method for coupling to dielectric resonators in microwave circuits is by proximity coupling to microstrip lines. This approach is equally applicable to DRAs as shown in figure. Mictrostrip coupling will excite the magnetic fields in the DRA to produce the short horizontal magnetic dipole mode. A metallic strip of definite width is etched on one side of a low loss dielectric substrate of known permittivity and thickness, the other side of which is metalized and grounded. An advantage of microstrip feed is that it is easier to fabricate, match and model. The feed is shown in Figure 1.4.

Coupling of EM energy and the input impedance are set by adjusting the lateral position of the DR with respect to the strip line. It is more convenient for the DRA arrays as well. One disadvantage of this feed is that at higher frequency, surface wave modes are also excited in the substrate which affects the radiation pattern and efficiency of the DRA. For lower permittivity values (necessary for DRAs requiring wide bandwidth), the amount of coupling is generally quite small.

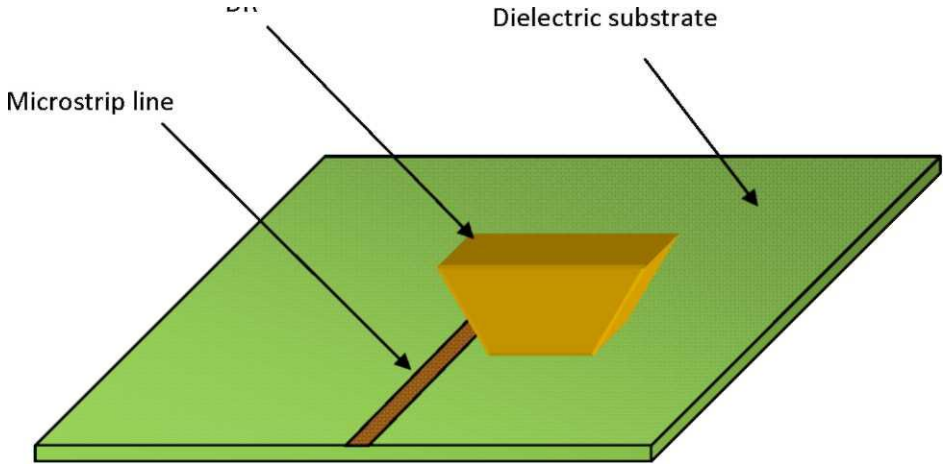

Figure 3.4: Microstrip line fed DRA

3.7 COPLANAR SLOT FEEDS

Coupling to DRAs can also be achieved using co-planar feeds. Figure shows a ITDRA coupled to a co-planar loop. The coupling level can be adjusted by positioning the DRA over the loop. The coupling behavior of the co-planar loop is similar to that of the coaxial probe, but the loop offers the advantage of being non obtrusive. By moving the loop from the edge of the DRA to the centre, one can couple into either the HE_{11}§ mode or the TE_{011} mode of the cylindrical DRA [17, 26]. A coplanar slot can also be used to feed the DRA as shown in figure.

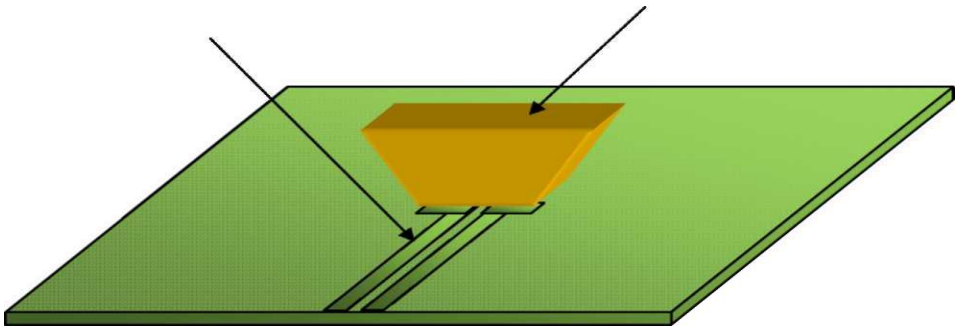

Figure 3.5: Co-planar slot feed DRA

3.8 WAVE GUIDE FEED

The primary advantage of a waveguide is that it is extremely less lossy in the millimeter wave band. Since the wave is completely guided within the metallic structure, there is no threat of radiation loss when used as a feed line. As both the waveguide and DR are very low-loss, they form an excellent combination for low-loss millimeter-wave communication systems. Coupling to the DR can be achieved through

a probe or a slot. A waveguide probe fed DRA is shown in Figure 1.6.

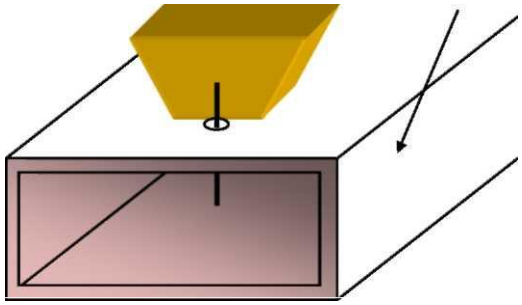

Figure 3.6: Waveguide probe fed DRA

CHAPTER 4:DIIFERENT DR GEOMETRIES

One of the attractive features of a DRA is that it can assume a number of shapes. Moreover the mode of operation and performance of a DRA can be varied by selecting a DR with desired structure. Hence a number of DRA geometries have already been tried experimentally. The first systematic, theoretical, and experimental study was made on cylindrical disk DRA geometry. Later geometries such as split cylinder, sectored cylinder, cylindrical rings, metallized DRAs, triangular, rectangular, notched rectangular DRA, chamfered DRA, conical, elliptical, spherical, hemispherical, spherical cap, tetrahedral, perforated DRA, stepped DRAs, and hybrid DRAs, have been reported. It was found that DRAs operating at their fundamental modes radiate like an electric or magnetic dipole, which depends on the mode of excitation and geometry of the bulk dielectric material. Geometries like conical, stair, stacked triangular etc emerged for dualband or wideband applications while those like cross, elliptical,hexagonal, cylindrical-comb etc emerged for circular polarization applications. Figure 2.1 shows the DR geometries, explained so far. Though several geometries have been introduced, the most studied and common structures are still the cylindrical and rectangular DRAs because of the simplicity in their design, fabrication, and analysis.

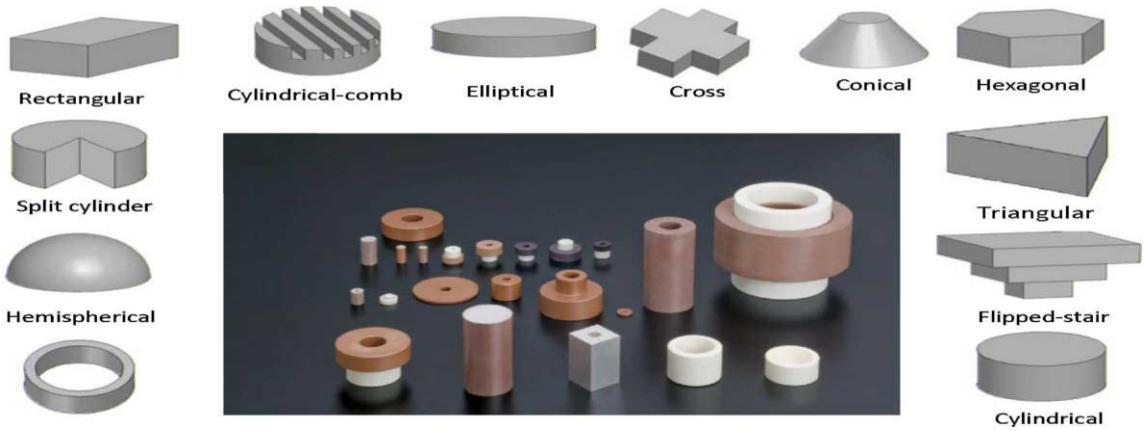

Figure 4.1: Different DR geometries used

4.1 CHARACTERISTICS OF A DIELECTRIC RESONATOR

DIELECTRIC CONSTANT

The dielectric constant of a material under given conditions reflects the extent to which it concentrates electrostatic lines of flux. In other words, it is the ratio of the amount of electrical energy stored in a material by an applied voltage, relative to that stored in a vacuum. An important property of a dielectric material is its ability to support an electric field while dissipating minimal energy in the form of heat. The lower the dielectric loss, the more effective a dielectric material is.

The net flux density D can be expressed as

$$D = s E + P \qquad \text{.....} (11)$$

where E is the electric field intensity and P is the net polarization given by

$$P = £_0 ZE \qquad \text{.....} \quad (12)$$

Where % is the electric susceptibility. Now Eq. (11) becomes

$$D = s_Q(1+x)E = {}^{S}o^{S}r^{E} \qquad (13)$$

Now we define the relative permittivity as,

$$s, = 1 + X \qquad (14)$$

in the complex form,

$$^{S}r = {}^{S}r \sim J^{£}r \qquad (15)$$

In Eq. (15), the real part is called the dielectric constant and the ratio —— = tan *8* is calledthe dissipation or loss tangent of the dielectric.

Hence it is clear that the dielectric properties of a DR are resulted from the phenomenon called dielectric polarization that occurs when electromagnetic fields pass through them. A DR at rest contains randomly oriented permanent electric dipoles. Whenan external field is applied, the dipoles align themselves in the direction of the field andthe material is said to be polarized. For most materials P vanishes as E vanishes.

4.2 QUALITY FACTOR

The radiation Q-factor of the DRA is determined using [1]:

where*We* and $P_{rad}$are the stored energy and radiated power, respectively. These quantities are given by:

$$W_e = \frac{\varepsilon_o \varepsilon_r abd}{32}\left(1+\frac{\sin(k_z d)}{k_z d}\right)\left(k_x^2 + k_y^2\right) \quad (1)$$

$$P_{rad} = 10k_o^4 \left|\boldsymbol{p}_m\right|^2 \quad (2)$$

where$p_m$is the magnetic dipole moment of the DRA:

$$\boldsymbol{p}_m = \frac{-j\omega 8\varepsilon_o(\varepsilon_r - 1)}{k_x k_y k_z}\sin(k_z d/2)\hat{\mathbf{z}} \quad (3)$$

The impedance bandwidth (BW) of the DRA can be estimated from the radiation Q-factor using:

$$BW = \frac{S-1}{Q\sqrt{S}} \quad (4)$$

where*S* is the maximum acceptable voltage standing-wave ratio (VSWR). The above equations can be used to generate the graphs which plot the normalized Q-factor (Q_e) as a function of the DRA dimensions *d/b* for various values of dielectric constant and various values of *a/b*. The normalized Q-factor is defined as:$\mathcal{L}_r$

Thus these curves can be used to estimate the Q-factor of a DRA without having to rely on the preceding equations.

4.3 FABRICATION OF THE DIELECTRIC RESONATOR

The DR is fabricated through the mixed oxide or solid state route which is a time consuming process, involving many steps such as Mixing and Grinding, Calcination process, Pellet shaping, Sintering process and Surface finishing. During these processes we can minimize the free energy of the material and redistribute the atoms. The minimization involves the reduction of internal surface area and an increase in the grain size.

4.4 MIXING AND GRINDING

Here, the preparation of DR sample from $ZnTiO_3$ material is explained as an example as it is used for the work in this thesis. Titanates (TiO_2) have many uses in electronic and material industry due to its piezoelectric, ferroelectrics and other properties.

We start with the chemical equation of the compound **ZnTiO**3 which is

ZnO + TiO_2 **$ZnTiO_3$**or in terms of atomic weight,

(65.39 (Zn)+15.999(O)) gms of ZnO + (47.67(Ti)+2*15.999(O)) gms of TiO2 —

(65.39(Zn)+47.67(Ti)+3*15.999) gms of ZnTiO3

or

81.389 gms of ZnO + 79.668 gms of TiO2 ― 161.057 gms of ZnTiCh

This gives the fact that 1 gm of $ZnTiO_3$ requires 0.5053 gm of ZnO and 0.4947 gm of TiO_2. Thus the stochiometric quantities of ZnO and TiO_2 required for forming *N* gms of ZnTiO3 as the final product can be calculated easily. The next step is mixing for eliminating aggregates and/or reducing the particle size. The weighed powders of ZnO and TiO_2 are mixed well with 100-200 % of distilled water for about 12 hrs in a ball-mill, which is a motor-driven barrel that rotates on its axis. The barrel is filled with the ceramic beads made of alumina or silicon carbide that act as the grinding medium for the powder. The creamy mixer is then dried in an oven at a 100°C.

4.5 CALCINATION PROCESS

In this process the endothermic decomposition reaction is taken place. Any salt such as carbonate or hydroxide, decomposes, leaving an oxide as a solid product by liberating a gas. This process causes the interaction of the constituents by the interdiffusion of their ions and so reduces the extent of the diffusion that must occur during sintering in order to obtain a homogeneous body. The calcinations conditions are important factors determining the shrinkage of the pellet during the sintering. The thermal conductivity of powdered materials is always low, so that a sufficiently uniform temperature can only be obtained through a depth of a few centimeters when the period at maximum temperature is 1 or 2 hours in most cases. If compound formation is to occur during calcinating or firing, the matter of neighboring particles must inter-diffuse and the time taken to complete the process is proportional to the square of the particle size. Here the well mixed powder is taken in an alumina crucible and calcinated at a temperature of 1000°C in an electric muffle furnace, for 2 hrs.

4.5.1 PELLET SHAPING

After the calcination process, the powder is crushed well in an agate mortar to form finer powder and then, mixed well with 4 % of Poly Vinyl Alcohol (PVA), an organic binder. Mixing with the binder provides sufficient strength to resist the

disintegrating effect of small stress on the shaped pellets prior to sintering. Dry pressing is carried out in dye with movable top and bottom punches, made of hardened steel as shown in figure 2.2.

Figure 4.2: Photograph of Dyes used for ITDR and Cylindrical DR

The die used in this work is hexagonal in shape that can be used for fabricating hexagonal DR as well. After fixing the dye cavity on the bottom punch, one of the top punches is placed inside the cavity. To fabricate ITDR, the remaining void space in the cavity is filled with an adequate amount of free-flowing powder (already prepared) and the top punch is descended to compress the powder to a predetermined volume, to a set pressure (75-300 MPa). Highly polished dye and punch surfaces ensure reduced wall friction. Shapes with a uniform section in the pressing direction are the easiest to produceby dry pressing. The time taken on an automatic pressing machine varies from 0.2 secondfor pieces of diameter around 1 mm to 5 seconds for large complex shapes.

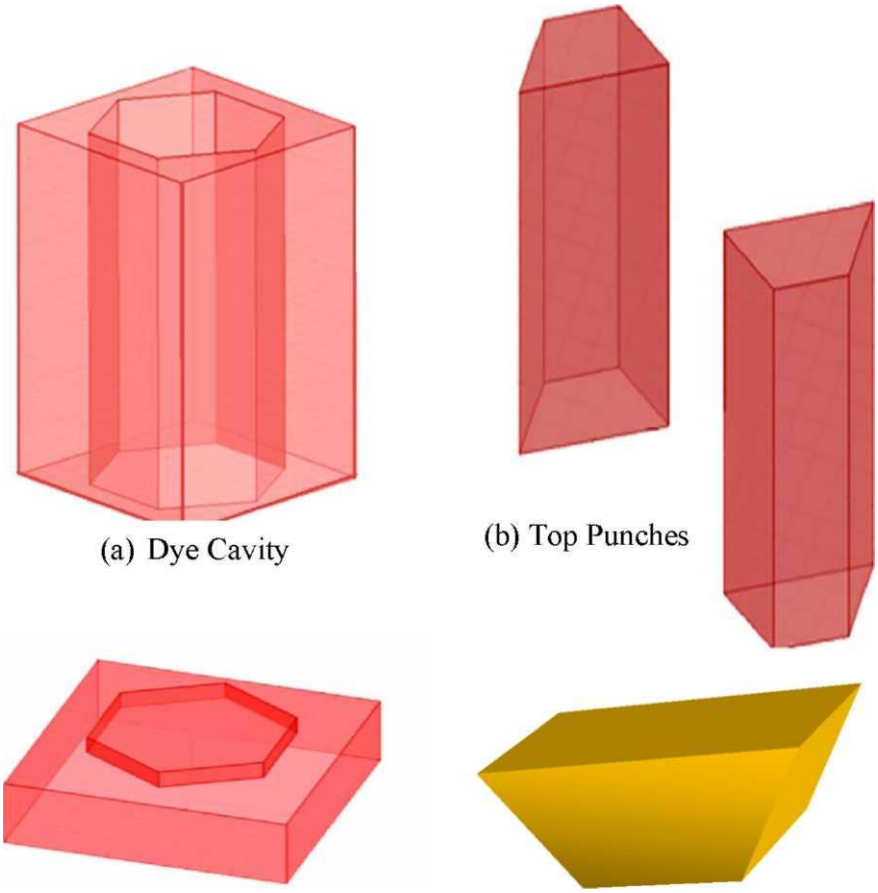

Figure 4.3: Schematic Sketches of the Dye and ITDR pellet

4.5.2 SINTERING PROCESS

Sintering converts the compacted powder in to a denser structure of crystallites jointed to one another by grain boundaries, at elevated temperatures below the melting point of the material. The energetic basis for sintering lies in the reduction of surface energy by transferring matter from the interior of grains along the grain boundaries to adjacent pores, which are eventually filled. Usually the powder compact is heated at fixed sintering temperature, held at this temperature for the required time and finally cooled at the room temperature. This is referred to as isothermal sintering. The organic binder is burnt out at the lower sintering temperatures. In the present case, isothermal sintering of the pellets, placed on an alumina slab at 1150°C for 5 hours is carried out after which it is cooled to the room temperature.

4.5.3 SURFACE FINISHING

Tool wear during the pellet shaping and variations in shrinkage during sintering and drying contribute to 1-2 % variation in the dimensions of the sintered pellets. For experimental studies, especially in the case of material characterisation, the surfaces of the pellets need to be as smooth as possible. Usually it is done by grinding and lapping the dense sample with tools consisting of silicon carbide, diamond powder etc. Here we use a silicon carbide water roof paper for finishing the pellets. A photograph of the final DR samples is shown in Figure 2.3.

Figure 4.4: Photograph of the fabricated DRs

4.5.4 MICROWAVE SUBSTRATES

Selection of substrates in microwave circuits is very important. Low loss substrates are very important at microwave bands. As frequency of operation increases, the loss tangent of the material used for substrates slightly increases, which in turn adversely affect the efficiency of the antenna. The power handling capability of the antenna depends on the substrate materials also. At high power certain substrate materials cannot withstand. A variety of substrate materials are available in the market. Flexible substrate materials are also available, so that the antenna can be mounted on curved surfaces. The selection of dielectric constant of the substrate depends on the application of the antenna and the radiation characteristics specifications. It is worth noting that surface waves will be excited in high dielectric constant substrates. This will generate spurious radiations in unwanted directions from the antenna. In this thesis

importance is given to compactness of the antenna structure. Prototype of antennas was fabricated on FR4 substrate which has a dielectric constant = 4.4, tan 5 = 0.02 and thickness = 1.6 mm.

4.6 CHARACTERIZATION METHODES OF DR

Dielectric constant and quality factor of the fabricated DRs are measured using the well-known cavity methods as described below.

4.6.1 Measuring Dielectric Constant using Hakki - Coleman Method

Depending on the operating principle, methods for measuring the complex permittivity of materials at microwave frequencies can be classified as (1) methods that depend on the standing wave field within the dielectric (2) methods that depend on transmitted waves or waves reflected from the dielectric and (3) resonance methods. When the material is available only in small volume, cavity perturbation techniques are suitable, but the measurement accuracy is limited to dielectric constants less than 10. Hakki and Coleman method is most suited when the ceramic samples have higher dielectric constant, and the method uses a dielectric post resonator for this purpose.

The measurement setup consists of a cylindrical DR puck sandwiched between two conducting plates (of infinite extent theoretically) to form a parallel-plate DR. This method restricts most of the stored energy to the dielectric and allows the experimental configuration to closely approximate the analytical model. If the distance between the two parallel plates is smaller than one-half wavelength, then the excited TE_{011} mode will not radiate and the sides of the resonator can be left open for providing the coaxial coupling probes. The maximum dimensions of the specimen are set by the diameter of

the shorting plates while the minimum dimensions by the diameter of the coupling probes. The setup is shown in Figure 2.4.

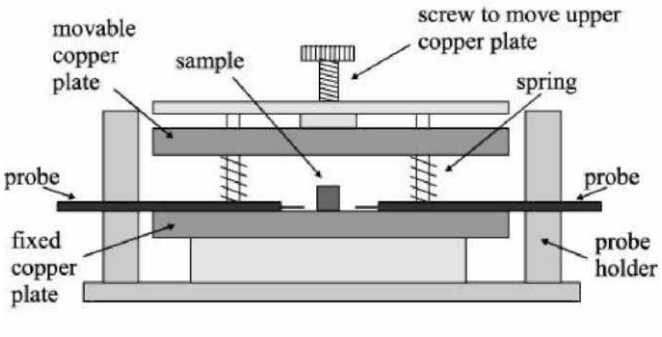

Figure 4.5 : Hakki-Coleman setup for measuring dielectric constant

4.6.2 Measurement of Quality factor using Cavity Method

Q-measurement methods are mainly of two types - time domain and frequency domain. Time domain methods mainly depend on measuring the decay time constant τ of the stored energy in the cavity at frequency *fo,* and by using the following relation.

$$Q_L = 2nf_eT \qquad (1)$$

Three useful frequency domain techniques are the reflection method, the reactance method and the transmission method. Transmission method is the simplest and requires a transmission type cavity as shown in Figure 2.5

As shown in the figure, a microstrip transmission line is fabricated on a dielectric substrate. The DR is coupled magnetically to the transmission line by placing it nearby it on the substrate. The lateral distance *d* between the strip and the centre of the DR determines the coupling coefficient between them. By properly adjusting d, the TE_{015} mode can be excited in the DR. In order to suppress the radiation losses, the entire structure is covered with a metallic cavity of dimensions at least 3 times the size of the DR, with a top plate that can be moved up and down using a screw. The shielding conditions affect the resonant frequency and the Q of the DR.

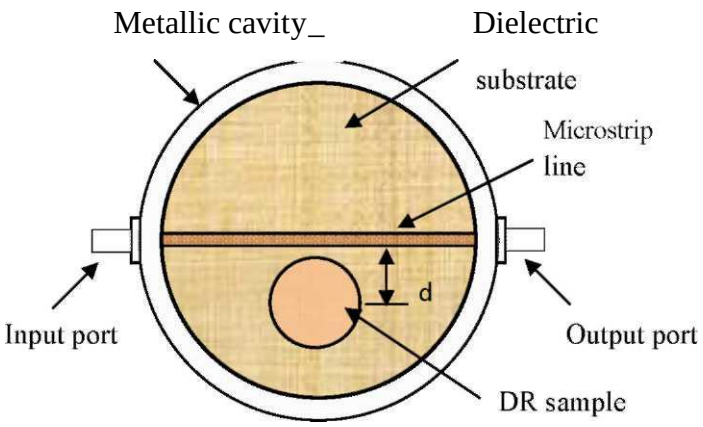

Figure 4.6: Top view of the transmission type cavity setup for Q-factor measurement

The degree of coupling is adjusted such that the transmission loss is of the order of -40 dB. By bringing the top metal plate close to the DR, the TE_{01}§ resonant frequency can be observed increasing, indicating that the stored energy in the cavity is predominantly magnetic. If the stored energy is electric, then a decrease in the resonant peak is expected. From the transmission coefficient ($|S_{21}|$) plot around the resonant frequency, the loaded and unloaded Q-factors-Q_L and Q,, respectively can be calculated as illustrated in Figure 2.6.

Here the parameter x is given by

$x=3 - 10.\log (1+10^{-01|S21|dB})$

Now the Q-factor is given by the well-known equation, $Q = -\frac{f}{Af}$

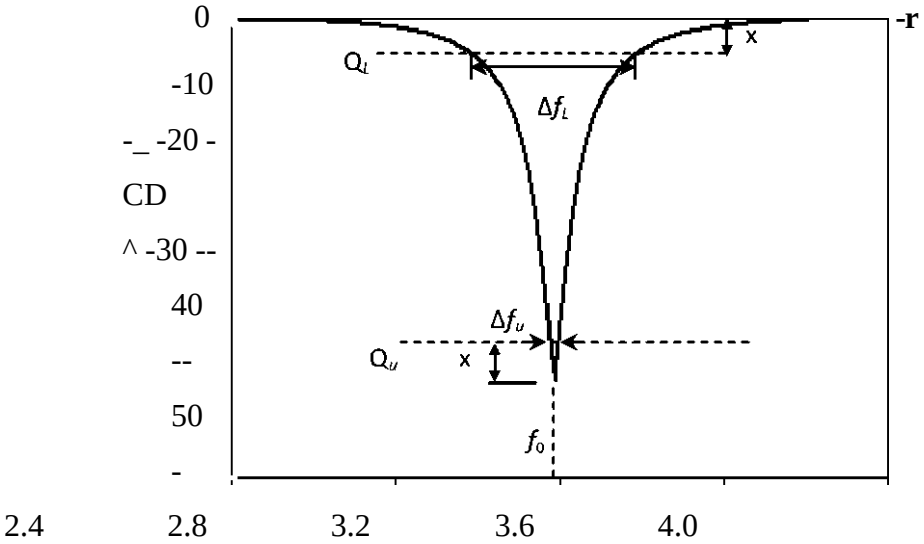

Figure 4.7: Measurement of Q-factor from the S_{21} curve

For the measurement of the temperature coefficient of resonant frequency (x_f), the Hakki-Coleman transmission cavity is placed in a temperature stable furnace with outlets for signal coupling. The temperature is varied over a desired range in discrete steps and the shift in the TE_{011} frequency is noted. Now $T_f$can be calculated as given by Eq. (28). Here 'f_0' is the TE_{011} resonant frequency at room temperature and 'Af_0' is the frequency shift for a temperature gradient of 'AT'. The $T_f$can be either positive or negative depending on whether the frequency is increasing or decreasing respectively with the rise in temperature.

T_f= f -^{f}o AT parts per million or ppm /^{o} C

Chapter 5: EXPERIMENTAL CHARACTERIZATION SETUP

Antenna characteristics such as return loss, radiation pattern and gain are measured using the HP8510C and associated setup. The indegeneously developed CREMA SOFT is used for the automatic measurement of the radiation properties using HP 8510C Network analyzer. The important systems used for the antenna characterization are Vector network Analyzer, Anechoic Chamber, Automated turn table etc.

5.1 HP 8510C VECTOR NETWORK ANALYZER

This is a sophisticated Vector Network Analyzer (VNA) from Hewlett Packard with time domain and frequency domain operation capability. The NWA can measure the magnitude and phase of the S parameters. The microprocessor based system can measure two port network parameters such as s_{11}, s_{12}, s_{21} and s_{22} very accurately. The in built signal processing algorithms of the network analyzer process the transmit and receive data and finally displays the measured values in many plot formats. The schematic of the VNA.

The network analyzer consists of a microwave generator, S parameter test set, signal processor and the display unit as illustrated in Fig. 5.2. The synthesized sweep generator HP 83651B uses an open loop YIG tuned element to generate the RF stimulus. It can synthesize frequencies from 10 MHz to 50 GHz. The frequencies can be set in step mode or ramp mode depending on the required measurement accuracy.

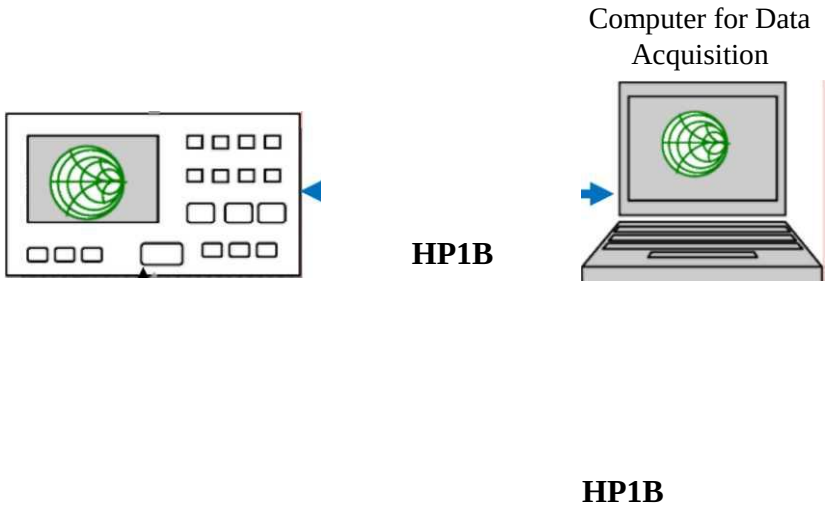

Figure 5.1: Schematic diagram of HP 8510C vector network analyzer set up used for the characterization of the antennas

The antenna under test (AUT) is connected to the port of the S-parameter test set HP8514B and the forward and reflected power at the measurement point is separated and down converted to 20MHz using frequency down converter. It is again down converted to lower frequency and processed in the HP8510C processing unit. All the systems discussed above are interconnected using HPIB bus.

A computer interfaced to the system is used for coordinating the whole operation remotely. Measurement data can be saved on a storage medium using it.

5.2 ANECHOIC CHAMBER

The anechoic chamber provides a quiet zone needed to simulate space environment required in pattern measurements. The absorbers used for building the chamber are made from high quality, low-density form impregnated with dielectrically/ magnetically lossy medium. The wall of the chamber (24' X 12' X 10') used for the measurements is properly shaped (tapered chamber) and covered with carbon black impregnated poly urethene (PU) foam based pyramidal, wedge, or flat absorbers of appropriate sizes. The PU foam structure gives the geometrical impedance matching while the dispersed carbon gives the required attenuation (up to -40 dB) for a wide frequency (500 MHz to 18 GHz) range. The chamber is made free of EMI by surrounding with thin aluminium sheet.

5.3 TURN TABLE ASSEMBLY FOR FAR FIELD RADIATION PATTERN MEASUREMENT

The turn table assembly consists of a stepper motor driven rotating platform for mounting the Antenna Under Test (AUT). The in-house developed microcontroller based antenna positioner STIC 310C is used for radiation pattern measurement. The main lobe tracking for gain measurement and radiation pattern measurement is done using this setup. A standard wideband horn (1-18GHz) is used as receiving antenna for radiation pattern measurements. The in-housed developed automation software *'Crema Soft'* coordinates all the measurements.

5.4 MEASUREMENT PROCEDURE

The experimental procedures followed to determine the antenna characteristics are discussed below. The network analyzer in real practice is connected to large cables and connectors. The connectors and cables will have its losses associated at higher microwave bands. Thus the instrument should be

calibrated with known standards of open, short and matched loads to get accurate scattering parameters. There are many calibration procedures available in the network analyzer. Single port, full two port and TRL calibration methods are usually used. The two port passive or active device scattering parameters can be accurately measured using TRL calibration method. Return loss, VSWR and input impedance can be characterized using single port calibration method.

5.5 RETURN LOSS, RESONANT FREQUENCY AND BANDWIDTH

The return loss characteristic of the antenna is obtained by connecting the antenna to any one of the network analyzer port and operating the VNA in s11/s22 mode. The calibration of the port is done for the frequency range of interest using the standard open, short and matched load. The calibrated instrument including the port cable is now connected to the device under test. The frequency vs reflection parameter (s11/s22) values is then stored on a computer using the 'Crema Soft' automation software.

The frequency for which the return loss value is minimum is taken as resonant frequency of the antenna. The range of frequencies for which the return loss value is with in the -10dB points is usually treated as the bandwidth of the antenna. The antenna bandwidth is usually expressed as percentage of bandwidth, which is defined as

$$\%\ Bandwidth = \frac{bandwidth}{centrefrequency} * 100$$

At -10dB points the VSWR is ~2. This implies that at resonance the VSWR value approaches unity. The above bandwidth is sometimes referred to as 2:1 VSWR bandwidth.

5.6 FAR FIELD RADIATION PATTERN

The measurement of far field radiation pattern is conducted in an anechoic chamber. The AUT is placed in the quite zone of the chamber on a turn table and connected to one port of the network analyzer. A wideband horn is used as a transmitter and connected to the other port of the network analyzer. The turn table is controlled by a STIC positioner controller. The automated radiation pattern measurement process is coordinated by the *'Crema Soft'* software in the remote computer.

In order to measure the radiation pattern, the network analyzer is kept in S_{21}/S_{12} mode with the frequency range within the -10dB return loss bandwidth. The number of frequency points are set according to the convenience. The start angle, stop angle and step angle of the motor is also configured in the *'Crema Soft'*. The antenna positioner is boresighted manually. Now the THRU calibration is performed for the frequency band specified and saved in the CAL set. Suitable gate parameters are provided in the time domain to avoid spurious radiations if any. The *Crema Soft* will automatically perform the radiation pattern measurement and store it as a text file.

5.7 ANTENNA GAIN

The gain of the antenna under test is measured in the bore sight direction. The gain transfer method using a standard gain antenna is employed to determine the absolute gain of the AUT [46-47]. The experimental setup is similar to the radiation pattern measurement setup. An antenna with known gain is first placed in the antenna positioner and the THRU calibration is done for the frequency range of interest. Standard antenna is then replaced by the AUT and the change in S_{21} is noted. Note that the AUT should be aligned so that the gain in the main beam direction is measured. This is the relative gain of the antenna with respect to the reference antenna. The absolute gain of the antenna is obtained by adding this relative gain to the original gain of the standard antenna.

5.8 RADIATION EFFICIENCY OF DRA

The radiation efficiency n_{rad}describes the losses within the antenna structure. It is defined by the ratio of the radiated power P_{rad} over the power P_{in} going into the antenna terminal.

$$\text{Radiation Efficiency, } n = \wedge = \frac{P_{rad}}{P_{in}} = \frac{R_{rad}}{R_{rad} + R_{loss}} \qquad (3.27)$$

Where P_{rad}= power radiated

P_{in}= power fed to antenna (W) *Ploss*= power lost by the antenna (W) R_{rad}= radiation resistance of the antenna (Q) R_{loss}=loss resistance of the antenna (Q) For physically small antennas, the Wheeler cap method [48] is highly preferred for measuring the radiation efficiency. According to this method, if a radiation

shield is placed around the antenna so as to enclose the near fields of the antenna, the radiation resistance of the antenna is reduced to zero while the loss resistance and the stored energy remain the same as for the unshielded antenna [49]. When covering the antenna with a metal cap, the radiation is suppressed and the input power (proportional to the input resistance) is equal to the power loss (proportional to the loss resistance). Without the cap, the input power is equal to the radiated power plus the power loss (input resistance + loss resistance). The radiation efficiency of the antenna can be obtained from these two parameters.

5.9 ANTENNA UNDER TEST

The antenna under test (AUT) is the DRA designed using the fabricated ITDRs. Mainly three feeding methods are used. One with microstrip line feed alone and the other two are microstrip line feed with slotted ground plane. The slots provided in the ground plane are slightly different in shape for the use in Design 5-1 and Design 5-2 as would be seen in section 4.5.1 and 4.5.2 in chapter 4. The feed with substrate is shown in the figure.

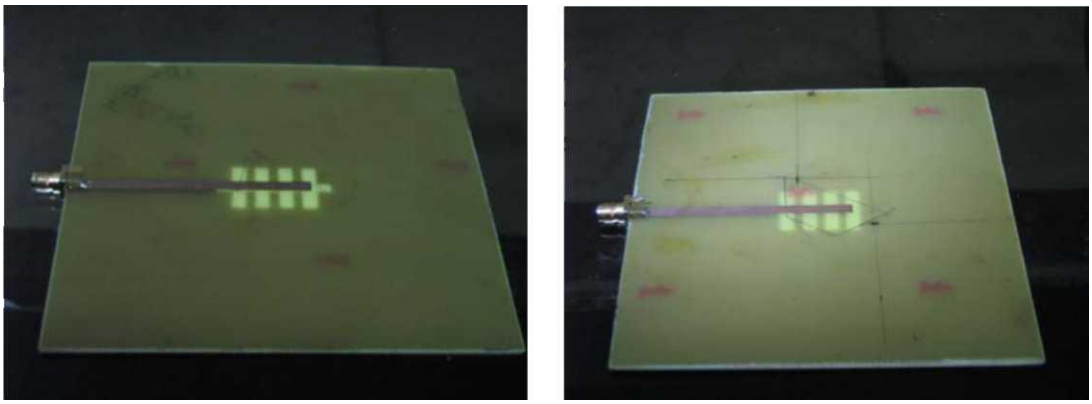

(a)

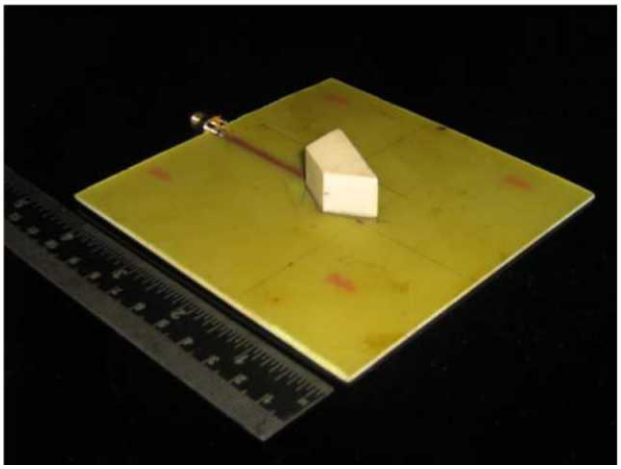

(c)

Figure 5.2: Photographs of the **(a)** feed used in Design 5-1 **(b)** feed used in -

Design 5-2 and **(b)** the antenna configuration with microstrip feed alone.

5.10 HFSS

HFSS is a commercial finite element method solver for electromagnetic structures from Ansys. The acronym originally stood for **high frequency structural simulator**. It is one of several commercial tools used for antenna design, and the design of complex RF electronic circuit elements including filters, transmission lines, and packaging. It was originally developed by Professor ZoltanCendes and his students at Carnegie Mellon University. Prof. Cendes and his brother Nicholas Cendes founded Ansoft and sold HFSS stand-alone under a 1989 marketing relationship with Hewlett-Packard, and bundled into Ansoft products. After various business relationships over the period 1996-2006, H-P (which became Agilent EEsof EDA division) and Ansoft went their separate ways: Agilent with the critically acclaimed FEM Element and Ansoft with their HFSS products, respectively. Ansoft was later acquired by Ansys.

By performing the following tasks in HFSS we reached our goal:

- ✓ Draw a geometric model.
- ✓ Modify a model's design parameters.
- ✓ Assign variables to a model's design parameters.
- ✓ Specify solution settings for a design.
- ✓ Validate a design's setup.
- ✓ Run an HFSS simulation.
- ✓ Create a 2D x-y plot of S-parameter results.
- ✓ Create a field overlay plot of results.
- ✓ Create a phase animation of results.

The antenna is cavity-backed with an annular-slot-fed hemispherical dielectric resonator. The antenna feed is achieved by coaxial excitation across one side of an annular slot between the cavity and the DRA dielectric.

The first objective is to draw the antenna's cavity, which is created by first drawing a sphere and then splitting it into a hemispherical solid

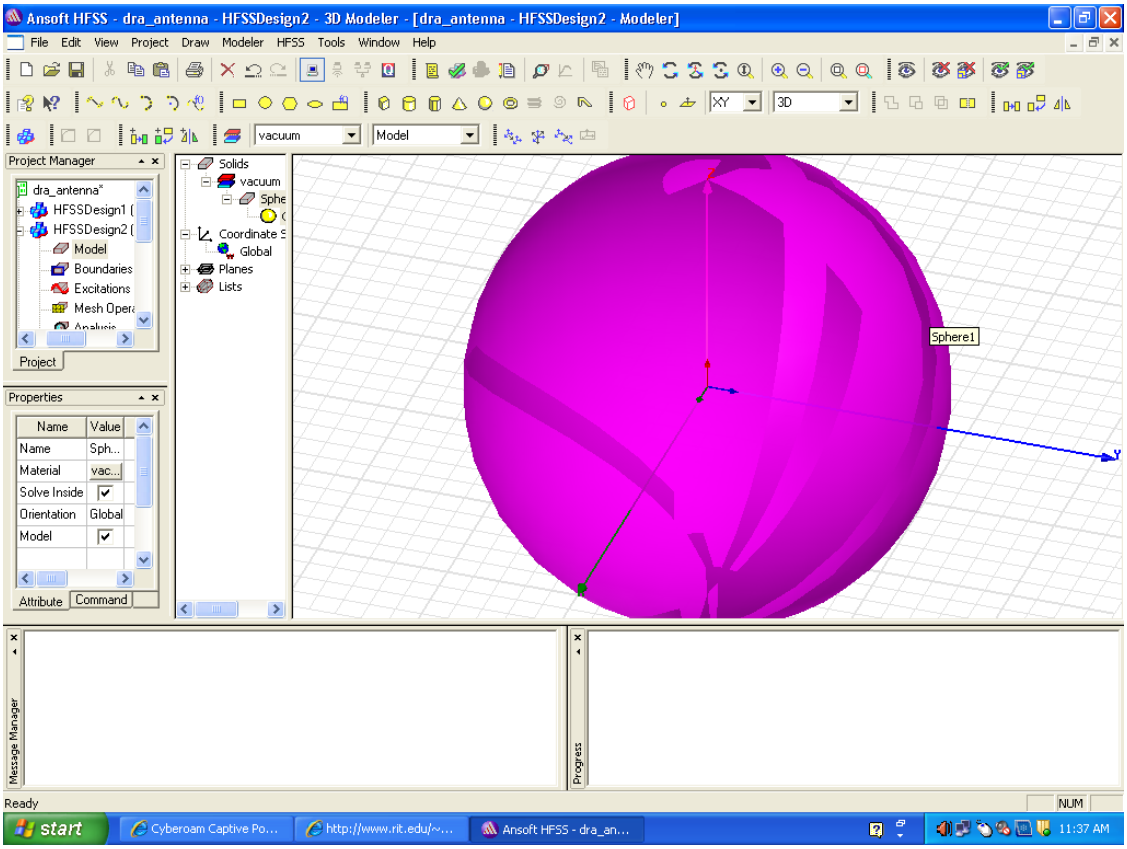

Figure 5.3: spherical cavity of the antenna

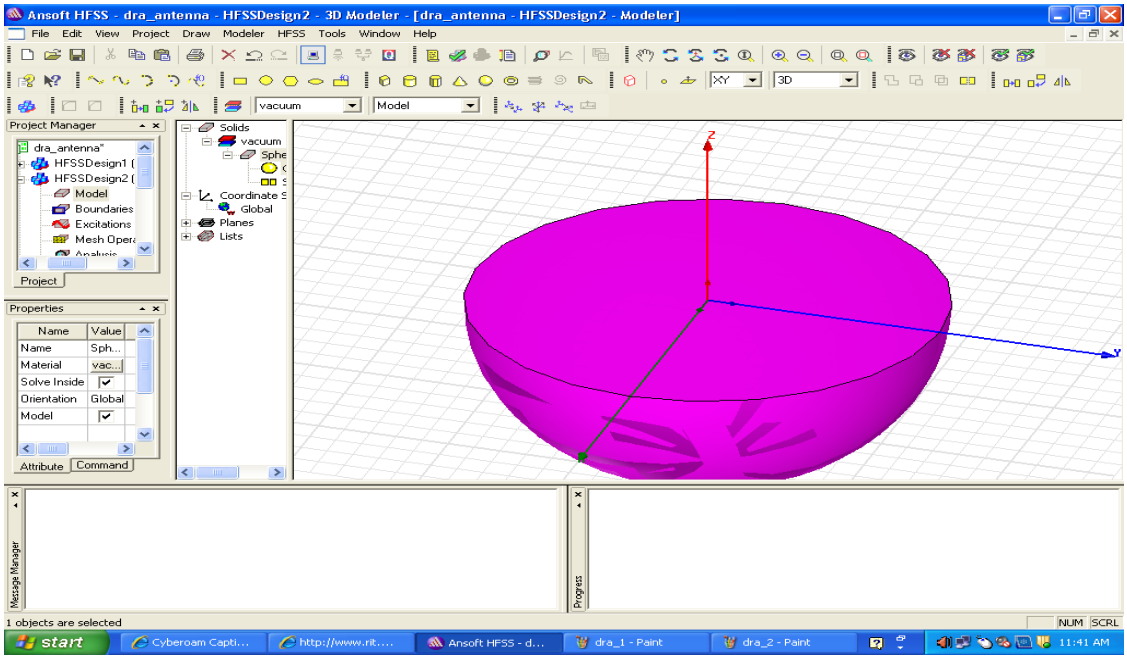

Figure 5.4: hemisphere

Draw the DRA

Now, the dielectric resonator (DRA) object.

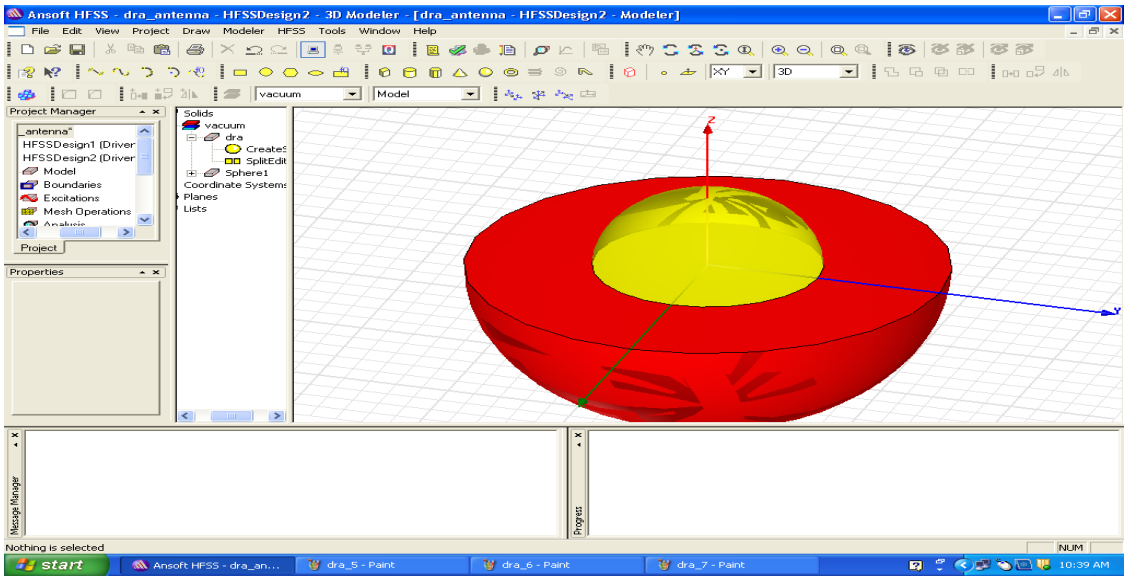

Figure 5.5: object of the DRA

Create the Annular Feed Ring In this antenna model, the annular feed ring is the controlled aperture through which the E-fields will radiate. “Setting Up the Problem”, assign a perfect H boundary to the annular feed ring to allow the E-fields to radiate through it.

Next, create the antenna’s annular feed ring, which is the result of subtracting one circle from another.

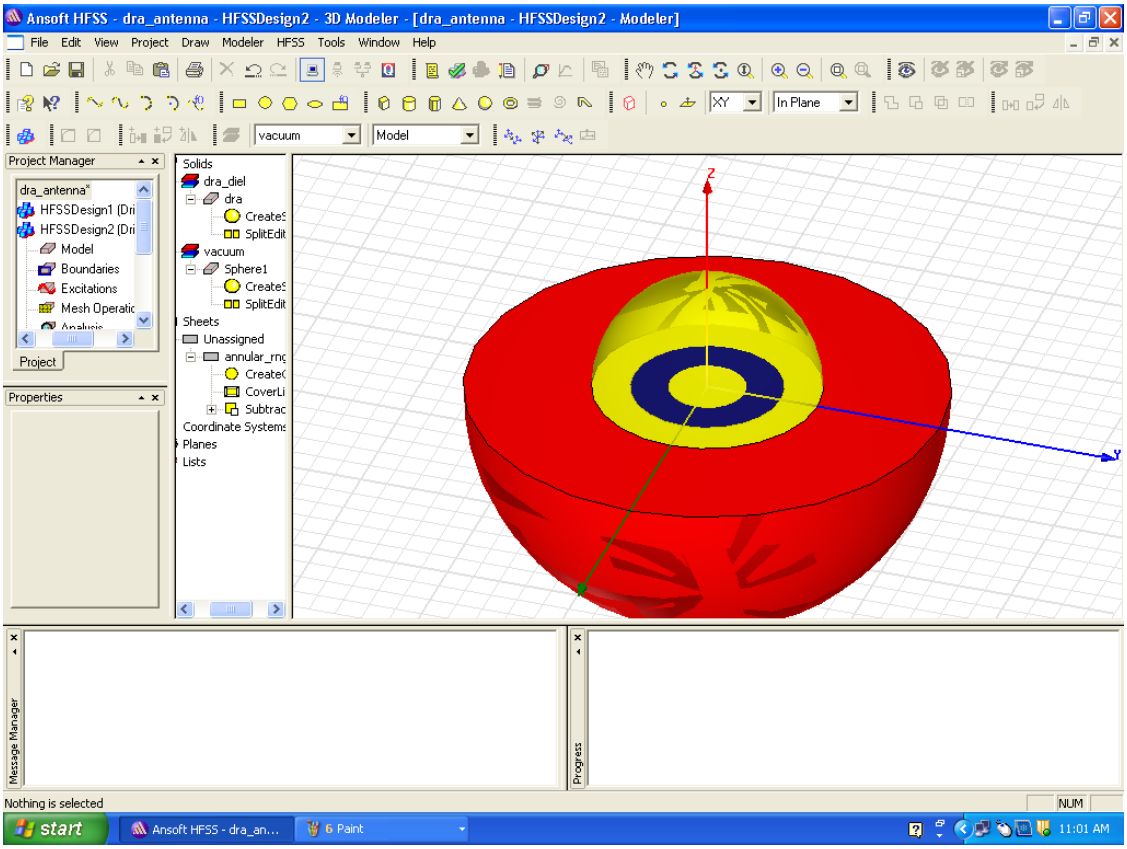

Figure 5.6: annular feed ring

Draw the Air Volume

To analyze radiation effects, create a virtual object that represents

the radiation boundary. For this antenna model, create a radiation-transparent air volume surface sufficiently far from the model. Next, draw a regular polyhedron with 18 segments to represent this virtual object. Setting Up the Problem, assign a radiation boundary to this object.

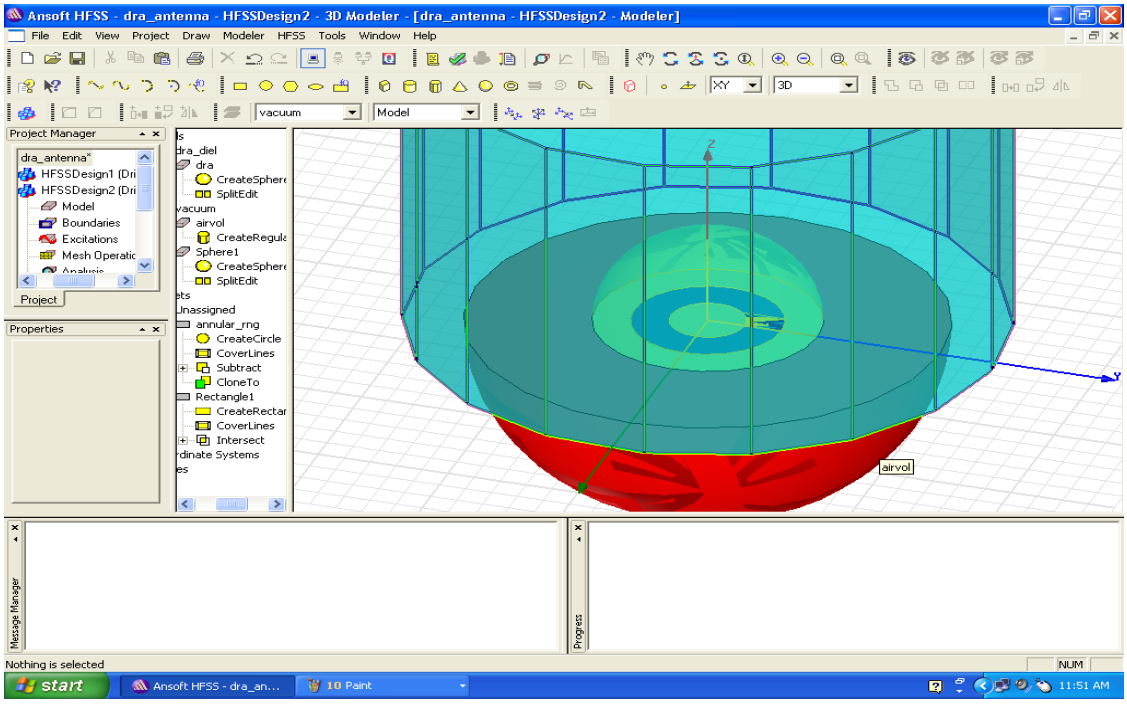

Figure 5.7: Air Volume

Set Up Boundaries and Excitations

Now objects of the antenna model are created and defined their properties, define the boundary and excitation conditions. These conditions specify the excitation signals entering the structure, the behavior of electric and magnetic fields at various surfaces in the model, and any special surface characteristics.

Boundary Conditions

Boundaries specify the behavior of magnetic and electric fields at various surfaces. They can also be used to identify special surfaces —such as resistors— whose characteristics differ from the default.

The following four types of boundary conditions will be used for this antenna problem:

Radiation This type of boundary simulates an open problem that allows waves to radiate infinitely far into space, such as antenna designs. HFSS absorbs the wave at the radiation boundary, essentially ballooning the boundary infinitely far away from the structure. In this antenna model, the air volume object is defined as a radiation boundary.

Perfect E This type of boundary models a perfectly conducting surface in a structure, which forces the electric filed to be normal to the surface. In this antenna model, the *bottom* face of the air volume object is defined as a perfect E boundary.

Perfect H This type of boundary forces the tangential component of the H-field to be the same on both sides of the boundary. In this antenna model, the annular feed ring is the aperture that is assigned this boundary. Because the aperture is defined as a

perfect H boundary, the E-fields will radiate through it. If it was not defined as a perfect H boundary, the E-field would not radiate through and the signal would terminate at the aperture.

Symmetry In structures that have an electromagnetic plane of symmetry, such as this antenna model, the problem can be simplified by modeling only one-half of the model and identifying the exposed surface as a perfect H or perfect E boundary. For this antenna problem, a perfect H symmetry boundary is used

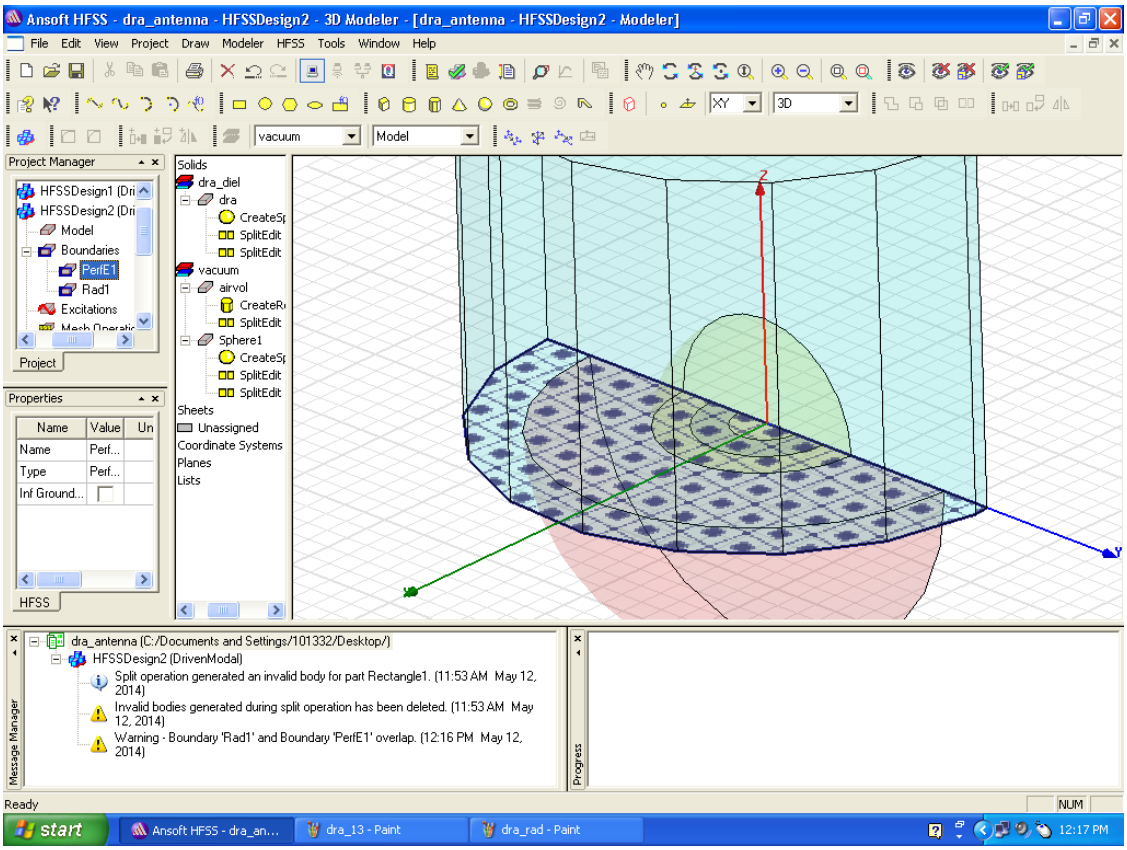

Figure 5.8: 'perfect e' boundary to the air volume

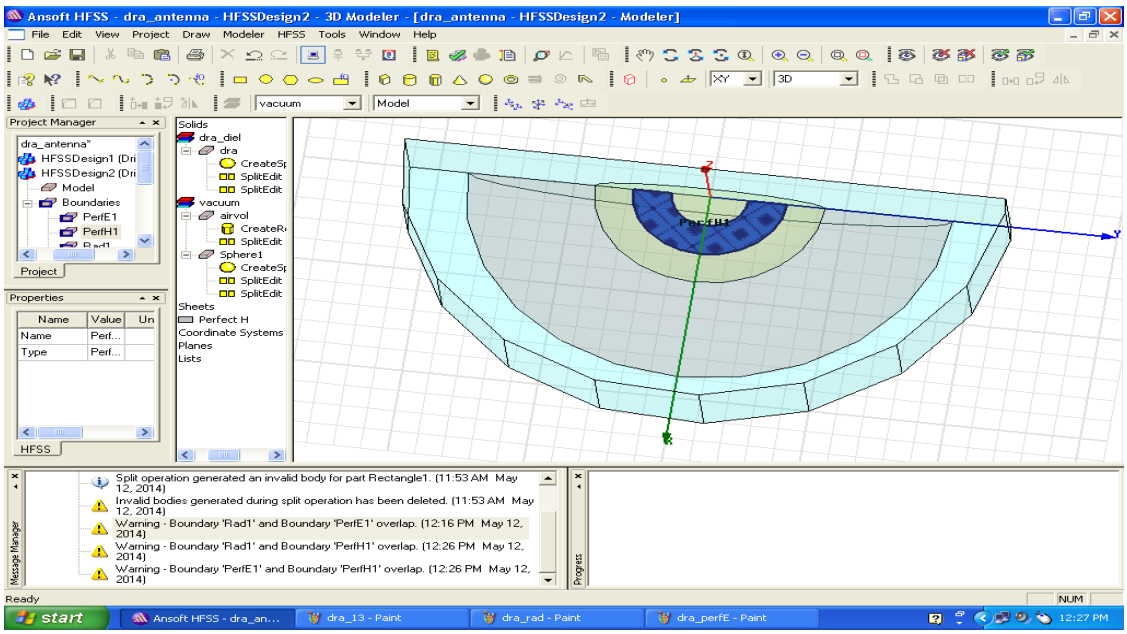

Figure 5.9: ‘perhect h’ boundary for to the annular ring

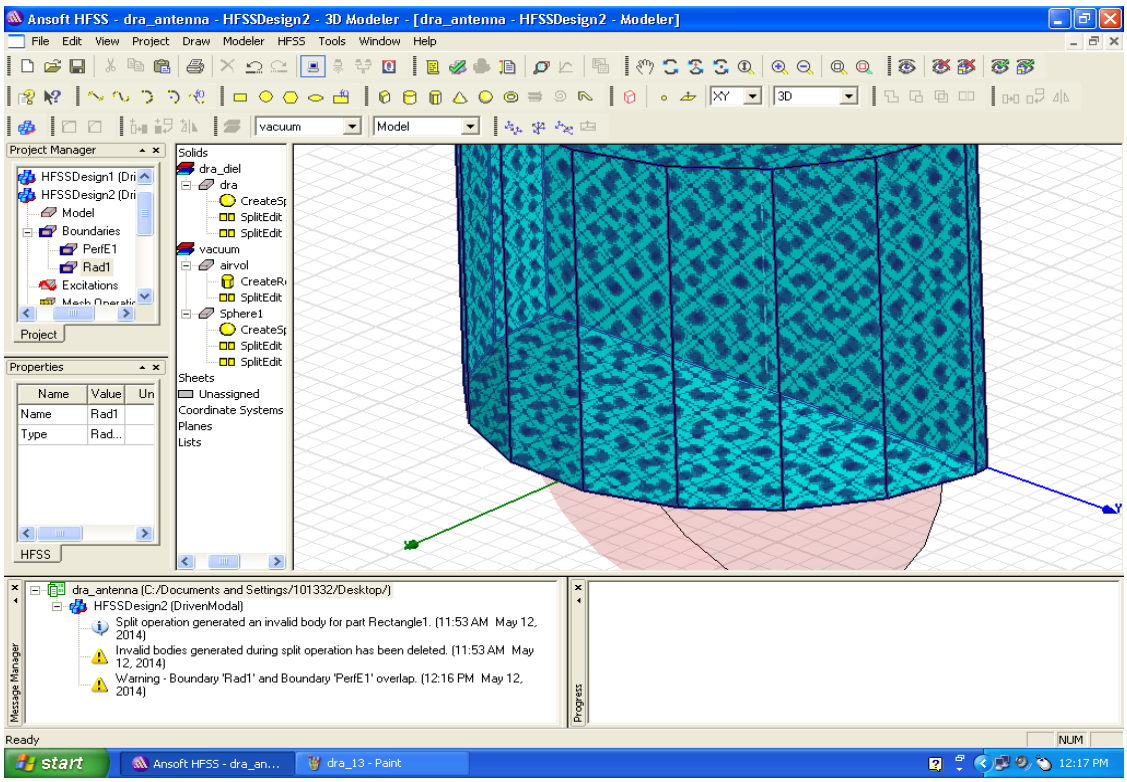

Figure 5.10: radiation boundary

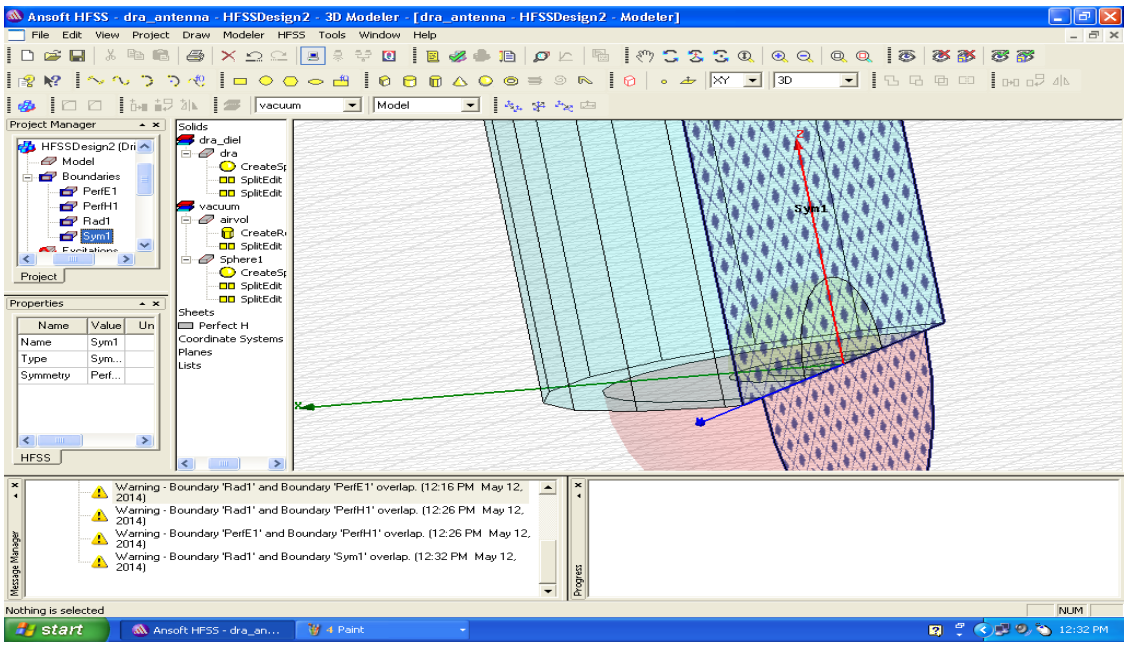

Figure 5.11: symmetry boundary

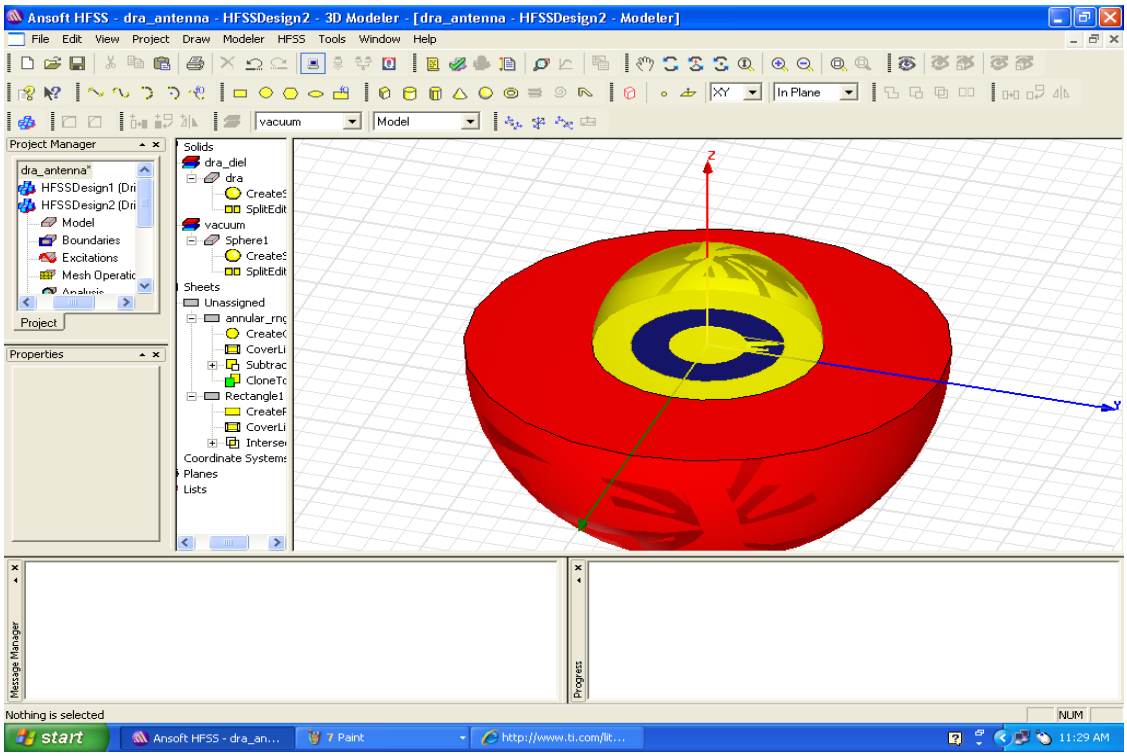

Figure 5.12: feed gap

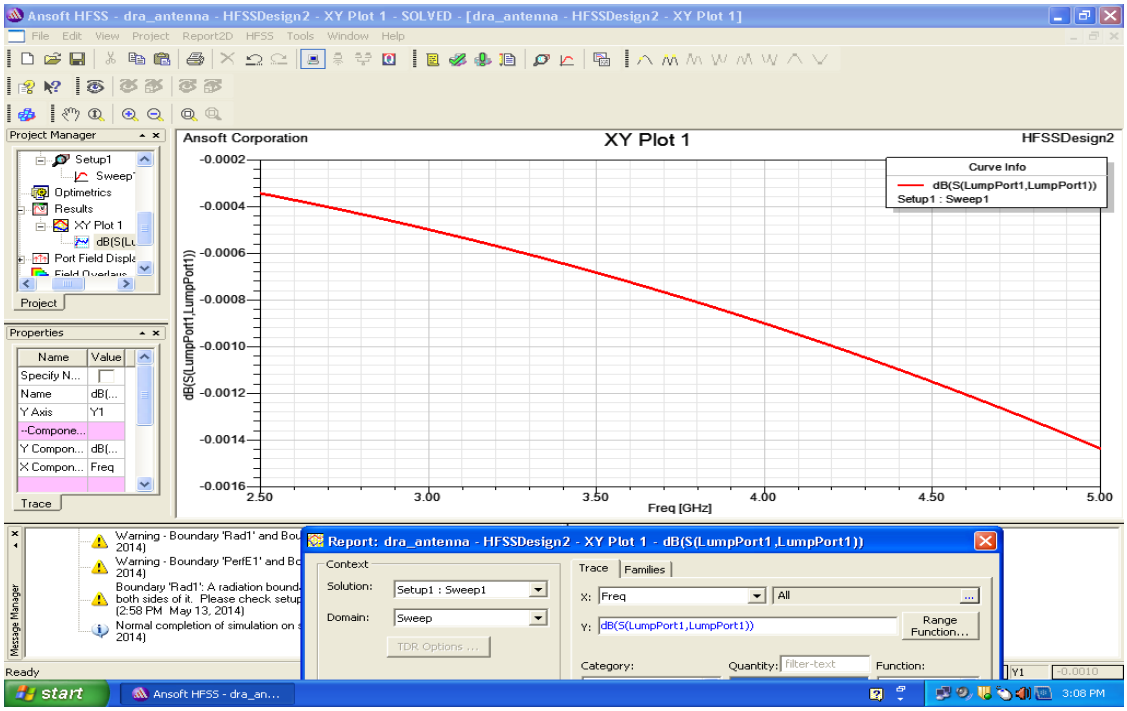

Figure 5.13: y axis: s parameter

x axis: frequency

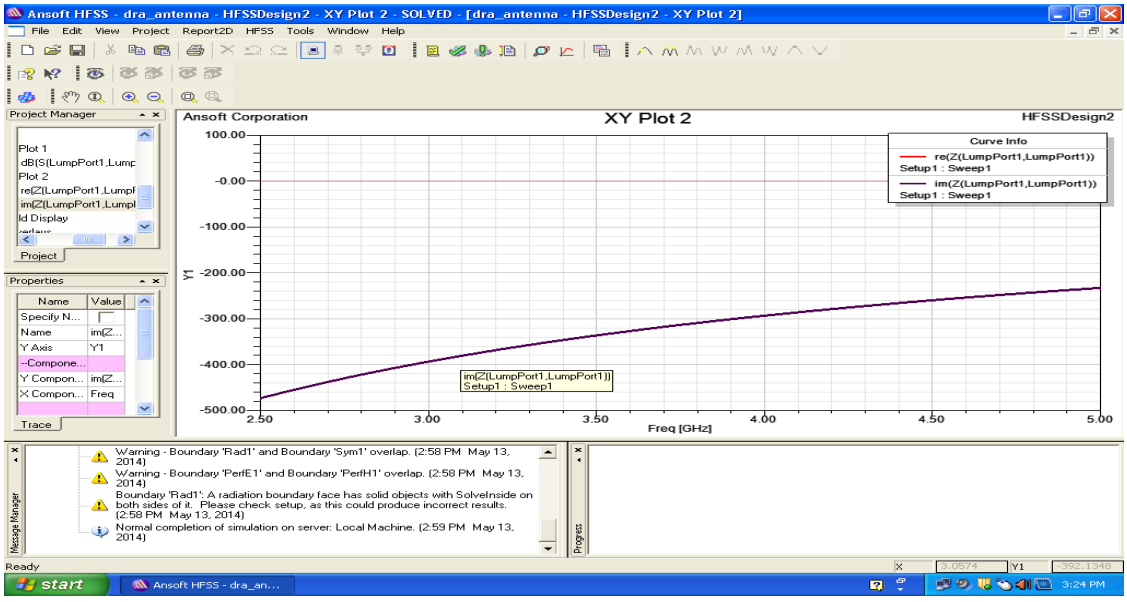

Figure 5.14: plot of z parameter

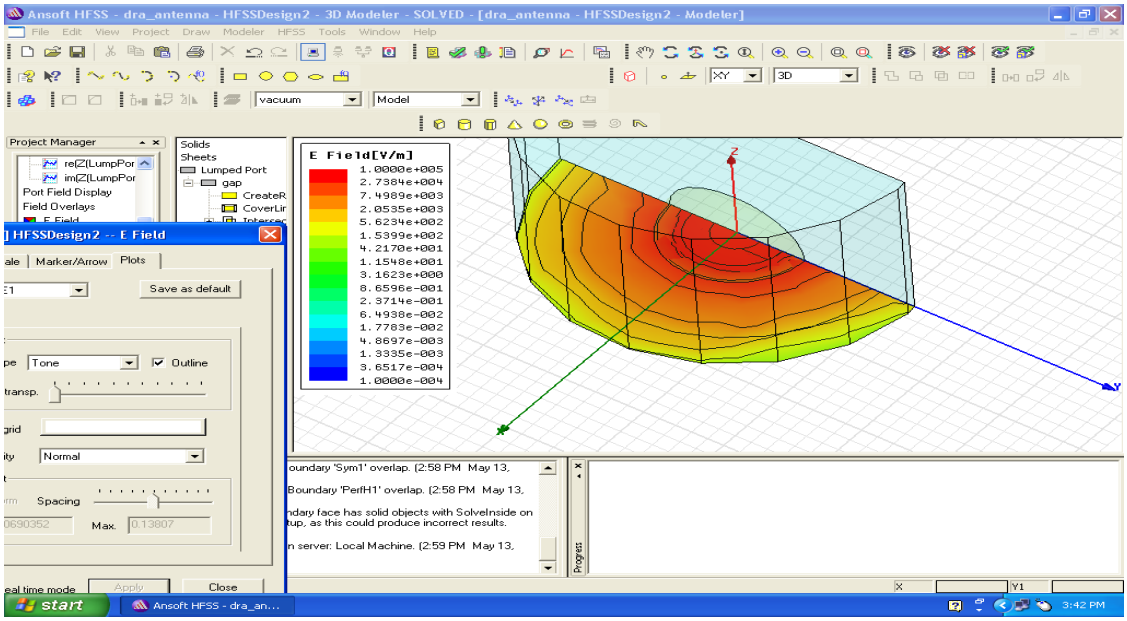

Figure 5.15: ‘ magnetic e’ plot

CHAPTER6:CONCLUSION

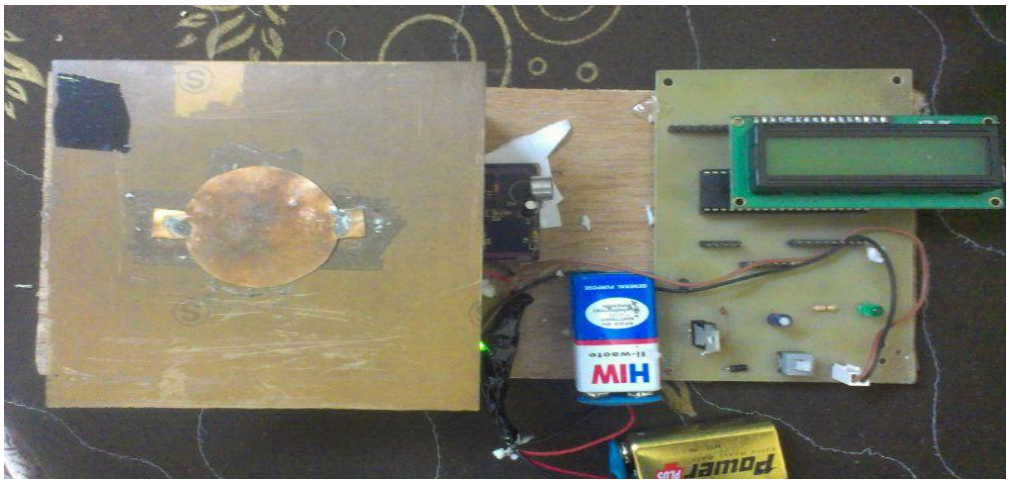

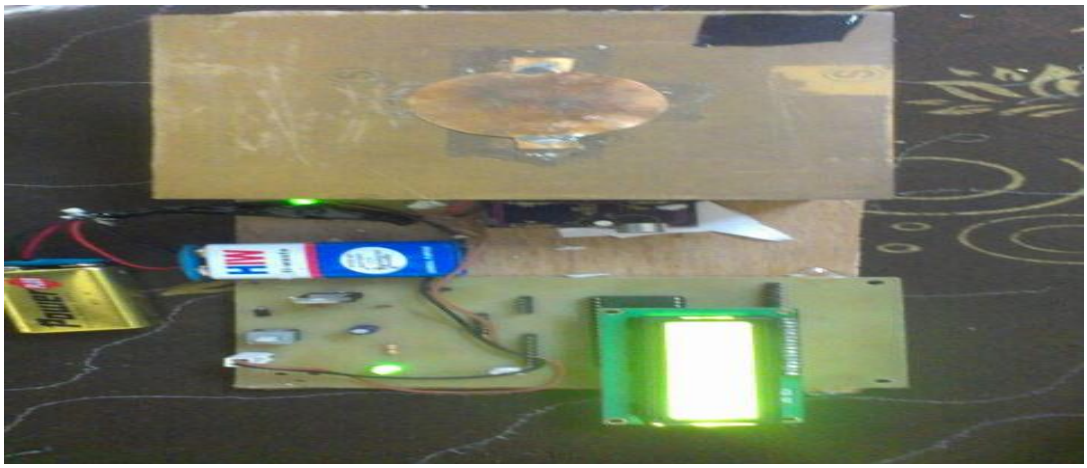

REFERENCES:

[1].A petosa, A. Ittipiboon, Y.M. M. Antar, D. Rossoe and M. Cuhaci, "Recent advances in dielectric resonator antenna technology," *IEEE Antennas Propagat. Mag.,* Vol.40 pp 35-48 June 1998.

[2]. Y. M. M. Antar and Z. Fan, "Theoretical investigations of aperture coupled rectangular dielectric resonator antenna," *Proc.Inst. Elect. Eng., PartH,* Vol 143, no.2, pp 113-118, April 1996.

[3].R. K. Mongia and A. Ittipiboon, "Theoretical and experimental investigations on rectangular dielectric resonator antennas" *IEEE Trans. Antennas Propagat.,* 1997, Vol.AP-45, no.9, pp 1348-1356.

[4].S. A. Long, M. McAllister, and L. C. Shen, "The resonant cylindrical cavity antenna," *IEEE Trans. Antennas Propagat.,* vol. AP-31, pp. 406-412, May 1983.

[5].M. McAllister, S. A. Long and G. L. Conway, "Rectangular dielectric resonator antenna," *Electron. Lett.,*vol. 19, pp. 219-220, Mar. 1983.

[6]. M. McAllister and S. A. Long, "Resonant hemispherical dielectric antenna," *Electron. Lett.,*vol. 20, pp. 657-659, Aug. 1984.

[7].A. A. Kishk, H. A. Auda, and B. C. Ahn, "Radiation characteristics of cylindrical resonant antennas with new applications," *IEEE Antennas Propagat. Soc. Newslett.,* vol. 31, pp. 7-16, Feb. 1989.

[8].R. K. Mongia, "Half-split dielectric resonator placed on a metallic plane for antenna applications," *Electron. Lett.,*vol. 25, pp. 462-464, Mar. 1989.

[9].K. W. Leung, K. M. Luk, K. Y. A. Lai and D. Lin, "Theory and experiment of a coaxial probe fed hemispherical dielectric resonator antenna," *IEEE Trans.*